Leishmania mitochondrial function and disease progression

Alexandra Maria Silva Soares Rodrigues
Mestrado em Bioquímica
Departamento de Química e Bioquímica
2017/2018

Orientadora
Margarida Duarte, Investigadora Auxiliar, Instituto de Investigação e Inovação em Saúde

Coorientadora
Ana Tomás, Professora Associada, Instituto de Ciências Biomédicas Abel Salazar

INSTITUTO DE INVESTIGAÇÃO E INOVAÇÃO EM SAÚDE
UNIVERSIDADE DO PORTO

U.PORTO
INSTITUTO DE CIÊNCIAS BIOMÉDICAS ABEL SALAZAR
UNIVERSIDADE DO PORTO

U.PORTO
FACULDADE DE CIÊNCIAS
UNIVERSIDADE DO PORTO

Todas as correções determinadas pelo júri, e só essas, foram efetuadas.
O Presidente do Júri,

Porto, _____/_____/_____

NORTE 2020
PROGRAMA OPERACIONAL REGIONAL DO NORTE
PORTUGAL 2020
UNIÃO EUROPEIA
Fundos Europeus Estruturais e de Investimento

The work was funded by the Norte-01–0145-FEDER 000012-Structured program on bioengineered therapies for infectious diseases and tissue regeneration, supported by Norte Portugal Regional Operational Program (NORTE 2020), under the PORTUGAL 2020 Partnership Agreement, through the European Regional Development Fund (FEDER)

Agradecimentos

Em primeiro lugar gostaria de agradecer à Doutora Margarida Duarte, orientadora desta dissertação, por me ter aceite no seu projeto. Obrigada por tudo o que me ensinou e por todas as críticas construtivas que me ajudaram a desenvolver profissional e pessoalmente.

Quero agradecer também à professora Doutora Ana Tomás, a minha coorientadora, que é a responsável pela minha entrada neste projeto devido à forma como me cativou através das suas aulas. Obrigada pela disponibilidade que sempre mostrou e pela atenção ao mais pequeno detalhe que permitiu melhorar consideravelmente este trabalho.

Queria também agradecer de uma forma especial à Tânia Cruz, por tudo o que me ensinou e por toda a ajuda que me deu dentro e fora do laboratório. E claro, obrigada por todas as boleias que me deste até casa! Obrigada Georgina Alves não só por me teres ensinado tudo o que sei sobre macrófagos mas também por todos os conselhos que me foste dando e pelos momentos de boa disposição.

Obrigada também a todas as meninas do grupo de Parasitologia Molecular do i3S: Maria, Inês, Teresa e Helena por todo o apoio e companheirismo. Um agradecimento especial à Sandra Marques pela frontalidade e disponibilidade para fazer uma leitura crítica desta tese.

Agradeço profundamente à minha família, especialmente aos meus pais, por estarem sempre lá para mim mesmo nas alturas mais difíceis. Obrigada por tudo, adoro-vos.

Por fim quero agradecer ao Pedro, o meu namorado e parceiro nesta jornada. Obrigada.

Resumo

A leishmaniose é uma doença tropical negligenciada responsável por mais de 20 000 mortes e 300 000 casos anualmente [1]. As opções de tratamento são limitadas e não há nehuma vacina disponível para humanos. O agente etiológico, *Leishmania*, é um parasita protozoário dimórfico extremamente adaptável. Como promastigotas, colonizam o trato digestivo da mosca-da-areia e são transmitidos a um vertebrado quando a mosca se alimenta do sangue deste. No novo hospedeiro, transformam-se em amastigotas e proliferam no fagolisossoma dos macrófagos, sendo capazes de estabelecer infecções crónicas. Parte do sucesso de *Leishmania* está certamente relacionado com o seu metabolismo mitocondrial, no entanto, os mecanismos e vias que permitem ao parasita prosperar no vertebrado estão longe de estarem elucidados. Estudos recentes demonstraram que a proteína mitocondrial p27 é essencial para a actividade do complexo IV da cadeia transportadora de electrões e também é crucial para a sobrevivência do parasita em modelos animais, nomeadamente em murganho [2]. Contudo, a sua função permanece desconhecida.

Neste trabalho tentamos compreender melhor o metabolismo mitocondrial de *L. infatum*, estudando mais detalhadamente a proteína p27, e verificámos que a atividade do complexo IV e o consumo de oxigénio eram superiores em parasitas $p27^{-/-}$ (sem p27) do que em parasitas WT. Apesar destes resultados serem diferentes daqueles apresentados em estudos com *L. donovani* [2], a carga parasitária de murganhos infetados com parasitas $p27^{-/-}$ foi significativamente mais baixa do que a de murganhos infetados com parasitas WT. Com base nos nossos resultados, propomos que a p27, quando associada com o complexo IV, reduz a sua atividade e induz um estado quiescente que permite a sobrevivência dos parasitas no hospedeiro vertebrado. Como tal, os parasitas são capazes de escapar mais facilmente ao sistema imunitário e resistir a flutuações de nutrintes, persistindo por longos períodos de tempo.

Palavras-chave:
Complexo IV, hospedeiro, infecção, *Leishmania*, metabolismo, mitocôndria, p27, virulência

Abstract

Leishmaniasis is a neglected tropical disease responsible for over 20 000 deaths and 300 000 new cases annually [1]. Treatment options are limited and no vaccine is available for humans. The etiological agent, *Leishmania*, is an extremely adaptable dimorphic protozoan parasite. As promastigotes, they colonize the digestive tract of a sand fly and are transmitted to a vertebrate when the fly takes a blood meal. There, they differentiate into amastigotes and proliferate in the hostile phagolysosome of macrophages, often establishing life-long infections. Part of *Leishmania*'s success is certainly related to mitochondrial metabolism, however, the exact mechanisms and pathways that allow it to prosper in the vertebrate host are far from being elucidated. The inner mitochondrial protein p27 shown to be essential for the increase in activity of Complex IV of the electron transport chain and parasite survival in a mouse model [2]. Yet, its function remains unclear.

While trying to get some insights on the mitochondrial metabolism of *L. infantum*, by pursuing further studies with p27, we observed that the activity of complex IV and oxygen consumption rates were higher in $p27^{-/-}$ parasites (depleted of p27) than in WT parasites. Although these results differ from a previous study in *L. donovani* [2], the parasite burden in mice infected with $p27^{-/-}$ parasites was significantly lower than in mice infected with WT parasites. Based in our results, we propose that p27 when associated with complex IV reduces enzyme activity inducing a quiescent state in the parasites, which allows them to survive in the vertebrate host. Consequently, parasites can more easily evade the immune response and endure nutrient fluctuations, persisting for long periods.

Keywords:

Complex IV, host, infection, *Leishmania*, metabolism, mitochondria, p27, virulence

Index

List of figures

List of tables

List of abbreviations

AB: add-back

ADP: adenosine diphosphate

APS: ammonium persulfate

ATP: adenosine triphosphate

BSA: bovine serum albumin

CCCP: carbonyl cyanide m-chlorophenylhydrazone

CL: cutaneous leishmaniasis

COX: cytochrome c oxidase (i.e. complex IV)

DAPI: 4',6-diamidino-2-phenylindole

DDM: n-dodecyl β-D-maltoside

DIG: digitonin

DNA: deoxyribonucleic acid

dNTPs: deoxynucleotide triphosphates

DMEM: Dulbecco's Modified Eagle's Medium

DMSO: dimethyl sulfoxide

EDTA: ethylenediamine tetraacetic acid

EGTA: ethylene glycol-bis(2-aminoethylether)-N,N,N′,N′-tetraacetic acid

ETC: electron transport chain

FBS: fetal bovine serum

HEPES: hydroxyethyl piperazineethanesulfonic acid

KC: Kupffer cells

KCN: potassium cyanide

LCCM: L929 cell conditioned medium

MAA20: medium for axenic amastigotes

MCL: mucocutaneous leishmaniasis

MEM: Minimum Essential Medium Non-Essential

mTXNPx: mitochondrial peroxiredoxin

NAD^+/NADH: nicotinamide adenine dinucleotide oxidized and reduced forms

NADPH: nicotinamide adenine dinucleotide phosphate reduced form

OE: over-expressing

ORF: open reading frame

PAM: protospacer adjacent motif

PBS: phosphate buffered saline

PCR: polymerase chain reaction

p.i.: post-infection

P_i: inorganic phosphate

PV: parasitophorous vacuole

PVDF: polyvinylidene difluoride

RNS: reactive nitrogen species

ROS: reactive oxygen species

rpm: revolutions per minute

RPMI: Roswell Park Memorial Institute

RT: room temperature

VL: visceral leishmaniasis

SDS: sodium dodecyl sulfate

TBS-T: tris-buffered saline and Tween 20

TCA: tricarboxylic acid

TEMED: N,N,N′,N′-tetramethylethylenediamine

TMPD: N,N,N′,N′-tetramethyl-p-phenylenediamine

Tris: tris(hydroxymethyl)aminomethane

WT: wild-type

Introduction

Parasite biology and disease manifestations

Parasitism consists in a symbiotic relationship between two organisms in which one – the parasite – is usually smaller and dependent on the host for survival. Parasites can have one or several hosts, be temporary or persistent, external or internal, obligatory or opportunists and belong to a wide range of taxonomical groups [3]. One of those groups, the order Kinetoplastida, includes obligatory parasitic protozoa characterized by the presence of a flagellum in at least one stage of its life cycle and the existence of extensive mitochondrial DNA, termed kinetoplast. This order includes the family Trypanosomastidae which encompass several species of the genera *Trypanosoma* and *Leishmania* [4,5].

Leishmania spp. are found in several countries in southern Europe, tropics and subtropics which include some parts of Asia, the Middle East, Africa, some parts of Mexico, Central America, and South America [6]. Transmission of parasites to vertebrate hosts occurs through a variety of species of sand flies from two major genus, *Phlebotomus* in the old world and *Lutzomyia* in the new world [4].

Leishmania parasites have two different morphological forms during their life cycle (figure 1): the promastigote (elongated cells measuring 15-20µm with a flagellum that can be up to three times the cell's length) and the amastigote (ovoid cells with 3-5µm and a rudimentary flagellum) [7]. Within the sand fly's gut the mobile promastigotes undergo a variety of developmental stages with varying biology. In the final stage they are termed metacyclic promastigotes and these are the non-dividing infective forms that are injected in a vertebrate host (e.g. humans and other mammals) when the sand fly takes a blood meal [8]. Once inside the new host, parasites are engulfed by macrophages and, normally, following phagocytosis, the phagosome matures through fusion with endosomes and later with lysosomes to destroy pathogens. However, *Leishmania* can influence this process, via disruption of phagosomal lipid microdomains, impairment of the assembly of the vesicular proton-ATPase and NADPH oxidase, which undermines fusion with vesicles, vacuolar acidification and generation of toxic ROS. It's inside this structure that promastigotes differentiate into amastigotes that can persist and divide intracellularly, acting as a reservoir for transmission [4,9–12].

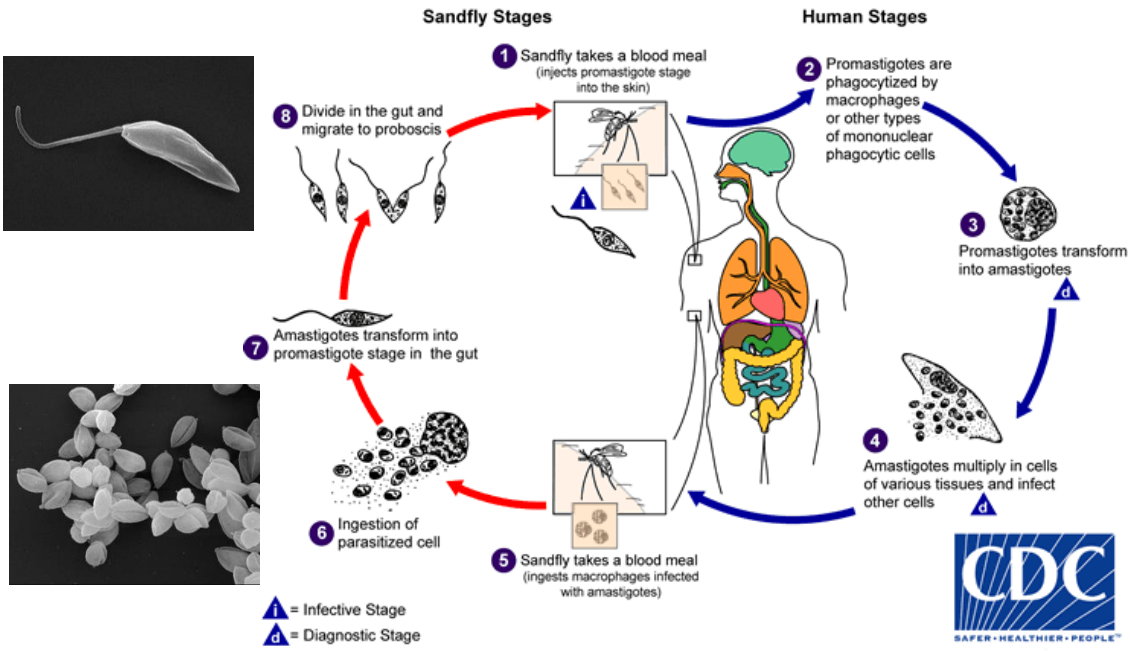

Figure 1. Morphological stages and life cycle of *Leishmania*. In the microphotographs to the left is possible to easily distinguish between the flagelated promastigotes (on top) and the rounded amastigotes (below). Promastigotes occupy the sand fly's gut (red arrows) and once injected into a vertebrate will transform into amastigotes (blue arrows). The different developmental stages of promastigotes are not represented in this image.
Life cycle scheme obtained from: https://www.cdc.gov/parasites/leishmaniasis/biology.html.
Microphotographies obtained from: http://www.cellimagelibrary.org/home

The PV can either harbor only one parasite or be occupied by many individuals [12]. Eventually, the macrophage ruptures and released parasites are phagocytized by other macrophages. This process will repeat itself until a fly feeds on the infected host, ingesting the amastigotes that will then differentiate into promastigotes in its gut, thus completing the cycle [7]. Although promastigotes can invade and survive in other cells like neutrophils, dendritic cells and fibroblasts, they don't appear to multiply. Little is known about the role of those other cells during the infection, but it has been hypothesized that they could act as refuges during an immune attack [9,13].

The array of diseases caused by these protozoans is known as leishmaniases, and they can be classified in three main types: cutaneous (CL), characterized by the presence of ulcers in the skin, mucocutaneous (MCL), with lesions in the mucous membranes (namely the mouth and nose) and visceral (VL), where internal organs like the liver and spleen are affected. The latter is the most severe and can be fatal if left untreated. Nevertheless, even the other forms of the disease can leave the host with dreadful scars and disfiguration. Hence, any form of the disease can be potentially debilitating and deadly. Most leishmaniases are zoonosis of wild or domesticated animals. VL usually involves canines (such as dogs or foxes) and CL often involves different types of mammals (rodents, sloths, marsupials, etc.) [14].

In Portugal, the etiological agent in most cases is *L. infantum* and the dog is the main host and reservoir. The link between canine and human leishmaniasis is not evident but the presence of infected dogs seems to be important for the maintenance of the disease among humans. It is estimated that 15-20 new cases of VL are diagnosed every year in the country. It used to be more common in children, but now the number of infected adults is rising, especially among immunocompromised individuals [15–17].

VL is a disease with considerable morbidity and mortality, causing over 20 000 deaths and an estimated 300 000 new cases annually, and more than 616 million people live in endemic areas at risk of infection [1]. Despite this, treatment options are limited, mainly due to the high toxicity of the existing drugs, resistant strains and high costs. No vaccine is available for humans, but for dogs two vaccines have been licensed [18]. To counter this lack of options, many populations of endemic areas resorted to leishmanization, the act of deliberately infecting a naïve person with an inoculum obtained from an infected person to provide immunity to future infections. This worked as a crude live vaccine and only for *L. major*, however, the practice has been discontinued due to the varying results and adverse effects [19].

Unveiling *Leishmania* biology, from the most basic metabolic process to the complex interaction between host and parasite, could hold the key to find new treatments by discovering the weakness of this ingenious parasitic protozoan.

Infection in the vertebrate host

A great number of aspects are thought to influence the outcome of *Leishmania* infections in a host, although the species of infecting parasite appears to be the decisive factor for the type of leishmaniasis that will develop. For example, *L. infantum* and *L. donovani* are causal agents of VL, whereas *L. major* causes CL [1].

This work will focus mainly on one of the species responsible for VL and their behavior in the vertebrate host. Visceral species of *Leishmania* infect mainly the liver and spleen, though these organs are not affected in the same manner. For instance, in mouse models, *L. donovani* and *L. infantum* amastigotes grow rapidly in the liver (figure 2a) for 20-28 days, and then start to decrease abruptly in the following month (this can vary among different mouse strains). In the spleen, this is not the case. The infection is not completely cleared and parasites can remain indefinitely inside the host (figure 2b) [20].

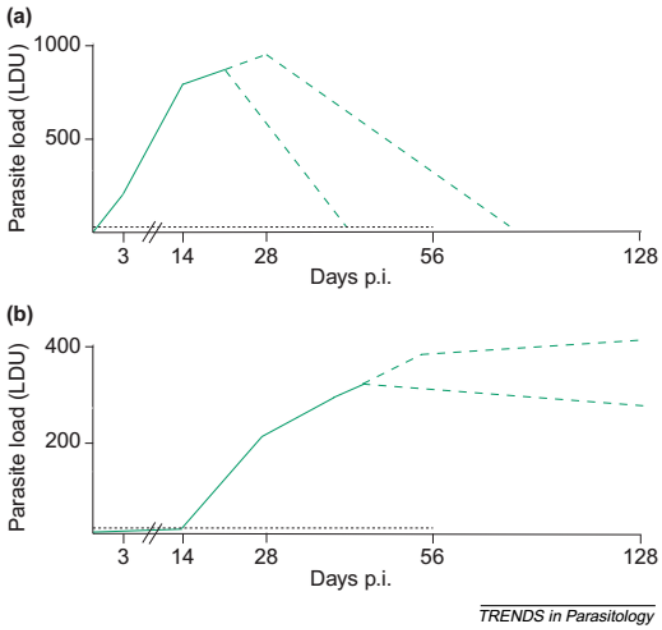

Figure 2. Examples of parasite load in mice infected with *L. donovani*. **(a)** Initially, in the liver, there is an exponential growth of amastigotes, followed by a decrease in parasite number due to the immune response. **(b)** In the spleen there is no evident replication in the first days and when replication begins it's not as fast and the parasite burden is lower when compared to the liver. The parasites are not fully cleared from this organ.
Broken black lines represent the limit of detection. Broken green lines represent variations among different studies. Adapted from [20]

What makes the parasite be contained in one organ but eliminated in the other? In the liver, resident Kupffer cells (KC) have a reduced ability to kill pathogens, and so, the parasite burden increases exponentially during the first days post-infection. To contain parasite numbers, inflammatory structures known as granulomas are formed. These consist of a center filled with infected KC and an outer layer of several types of immune cells. The concentration of inflammatory cytokines increases significantly in the granulomas, allowing the activation of anti-leishmanial mechanisms and the recruitment of T cells to clear the parasite [21].

In the spleen, during the first hours after infection, parasites are quickly removed from circulation by splenic macrophages and immune responses are mounted, namely antigen-specific T cell responses. Initially, this response is effective in restraining parasite growth, but between 14-21 days post-infection major structural changes occur, and consequently, immune dysfunction [22]. The splenic architecture crumbles (splenomegaly, disorganization of white pulp, hypertrophy of red pulp, etc.), T cell apoptosis increases and antigen response decreases. Tumor necrosis factor (TNF), produced by infected macrophages, is the main culprit for many of these events. Besides this, it contributes to IL-10 production, an anti-inflamatory cytokine that disables anti-leishmanial mechanisms and down-regulates the expression of co-stimulatory molecules, effectively establishing a chronic infection [21,22].

Despite this pattern, the pathogenesis of VL is complex and the manifestations can range from an ultimately fatal disease to asymptomatic infections. The factors determining which type of manifestation will develop in a host are still obscure [23].

Nevertheless, even asymptomatic infections have clinical and epidemiological importance, since the host can act like a reservoir for transmission and the disease can be reactivated (e.g. in an immunosuppressed host) [24–27].

Leishmania's energy metabolism

Leishmania parasites experience a wide range of environments with considerable variations in nutrient availability, pH and temperature. Yet, they are able to survive and thrive in distinct places like the digestive system of the fly and the hostile phagolysosome of macrophages, demonstrating that they are extremely adaptable organisms. To accomplish this, they have a metabolism that, despite sharing similarities with other eukaryotes, is more robust and unique. It differs from other trypanosomatids and even varies among the different morphological stages of the species [28–30]. For example, the extracellular trypanosomatid, *Trypanosoma brucei*, when infecting a vertebrate host, relies mainly on glucose, since it is abundant in the bloodstream. Thus, their energy metabolism is one of the simplest, as it is based mostly on glycolysis. In the insect host, amino acids will be the main carbon source, namely L-proline [31].

In contrast, *Leishmania* promastigotes inside the fly have an abundance of glucose to use as an energy source (besides blood, the sand fly also feeds on nectar), hence glycolysis will be their main metabolic pathway [32]. On the other hand, amastigotes have to rely on other compounds, mainly amino acids and fatty acids. Nonetheless, glucose is essential for *Leishmania* survival in any stage of its life cycle and when available it is the preferred energy source [33]. It constitutively expresses a series of transporters responsible for the uptake of, not only glucose, but also other hexoses (galactose and mannose), amino sugars and pentoses (ribose and xylose) [33]. Once internalized, sugars are catabolized via the glycolytic pathway. However, unlike in mammals, the first seven steps of glycolysis take place in a peroxisome-like organelle, the glycosome, that is only found in trypanosomatids (figure 3) [34,35].

The ATP and NAD^+ consumed during the first steps of glycolysis must be restored to maintain equilibrium. The import of phosphoenolpyruvate (PEP) into the glycosome and its fermentation into succinate or its decarboxylation to pyruvate help generate both ATP and NAD^+. These can also be restored through the glycerol-3-phosphate/dihydroxyacetonephosphate (G3P/DHAP) cycle that transfers electrons from the glycosome and the mitochondrion. This cycle also provides precursors for lipid biosynthesis [30].

The pyruvate produced at the end of glycolysis can either be converted into alanine and is then secreted or transported into the mitochondrion. Unlike mammals, *Leishmania* only has a single mitochondrion that can occupy up to 12% of the cell's volume. Still, this is a very dynamic organelle that can change its size and shape as the conditions and nutrient availability vary [36,37]. Once inside the mitochondrion, pyruvate can be transformed into acetyl-CoA and enter the tricarboxylic acid (TCA) cycle or be converted into acetate and secreted [28,38]. All the enzymes involved in the TCA cycle are expressed [30], though studies in *T. brucei* showed that these are mostly involved in non-cyclic pathways like reduction of malate to succinate, formation of citrate, and catabolism of amino acids [39]. By contrast, in *Leishmania*, the TCA cycle is predicted to be fully active [40].

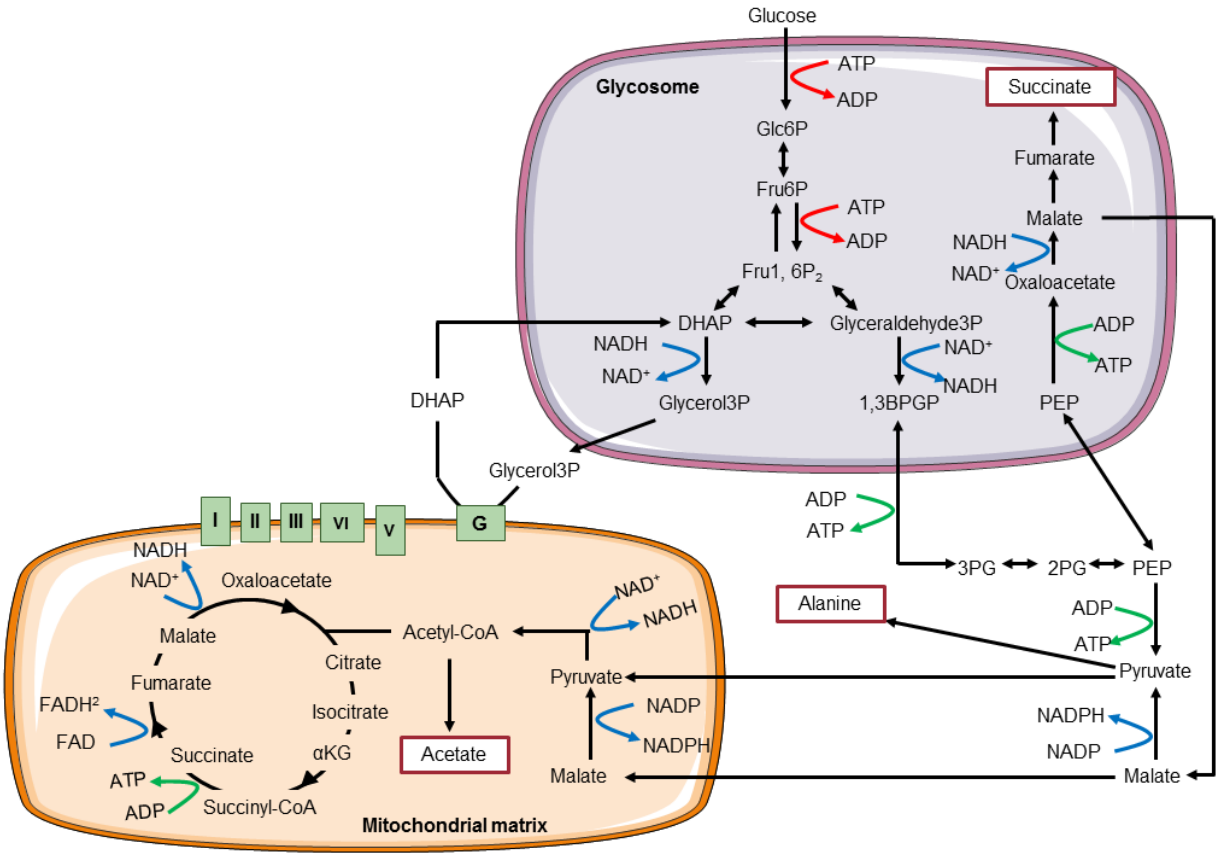

Figure 3. Simplified schematic summary of the major carbon metabolic pathways in *Leishmania*. End products are in white boxes with red contour. Abbreviations: I-IV, complexes of the respiratory chain; V, ATP synthase complex; G, glycerol-3-phosphate/dihydroxyacetonephosphate; NADH, reduced nicotinamide adenine dinucleotide; NAD^+, oxidized nicotinamide adenine dinucleotide; ADP, adenosine diphosphate; ATP, adenosine triphosphate; Glc6P, glucose-6-phosphate; $Fru1,6P_2$, fructose-1,6-biphosphate; DHAP, dihydroxyacetone phosphate; 1,3BPGP, 1,3bisphosphoglycerate; PG, phosphoglycerate; PEP, phosphoenolpyruvate; αKG, α-ketoglutarate
Adapted from [30]. Scheme made in part with images from https://smart.servier.com/

One peculiar type of energy metabolism, common to all trypanosomatids, is aerobic fermentation. These protozoans don't fully oxidize substrates and secret fermentation products (similar to those released by organisms placed in anaerobic conditions), however, they do it in the presence of oxygen as a final electron acceptor [28,41]. It appears that they cannot rely on a true fermentative process. In fact, *Leishmania* promastigotes have a low anaerobic capability [42]. They are resistant to anoxia to some extent, but end up in metabolic arrest with glucose consumption severely diminished. Succinate production does not seem to counter the lack of oxygen. Therefore, these parasites are largely dependent on the respiratory chain for the production of energy [42].

Like other eukaryotes, *Leishmania* has a classical electron transport chain (ETC) composed of four complexes inserted in the inner mitochondrial membrane, that must accept or donate electrons to the mobile electron carriers: ubiquinone and cytochrome c (figure 4) [43]. The first and largest enzyme of the respiratory chain is NADH dehydrogenase (Complex I) that receives electrons from NADH and transfers them to ubiquinone. Simultaneously, it pumps protons to the intermembrane space of the mitochondrion. The second, succinate dehydrogenase (Complex II), which is also part of the TCA cycle, is responsible for converting succinate into fumarate. The electrons formed during this reaction are taken up by ubiquinone again. No protons are pumped at Complex II [44]. Electrons from reduced ubiquinone are transferred to cytochrome c reductase (Complex III), which passes them to cytochrome c and then to cytochrome c oxidase (Complex IV, COX), which reduces oxygen to water.

As the electrons move along the respiratory chain, they release energy that is used to pump protons at the level of complexes I, III and IV from the matrix to the intermembrane space of the mitochondrion. This creates an electrical and pH gradient across the inner mitochondrial membrane allowing the protons to reenter into the matrix by passing through the ATP synthase complex (often called complex V). As this happens, conformational changes take place in this complex that allow the formation of ATP from ADP and P_i. This process is referred to as oxidative phosphorylation [44].

The process outlined above is the sequence of events that leads to energy production in cells. Nevertheless, trypanosomatids exhibit certain particularities that make their energy metabolism distinct from other eukaryotes. For example, the activity of complex I has long been debated with some researches arguing that this complex may be absent or have very little activity in some trypanosomatids. Indeed, trypanosomatids contain a type II NADH dehydrogenase (NDH2) and a NADH-dependent fumarate (mFRD) which could act as alternatives to complex I, although this

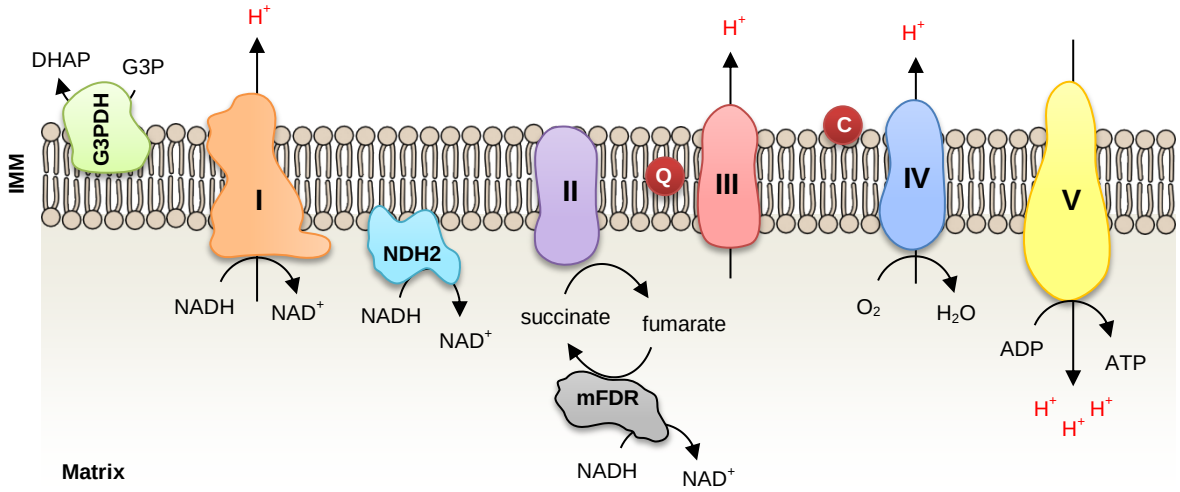

Figure 4. Schematic representation of oxidative phosphorylation in *Leishmania*. Abbreviations: I-IV, complexes of the respiratory chain; V, ATP synthase complex; IMM, inner mitochondrial membrane; G3PDH, Glycerol-3-phosphate dehydrogenase; NDH2, type II NADH-dehydrogenase; mFRD, mitochondrial fumarate reductase; NADH, reduced nicotinamide adenine dinucleotide; NAD^+, oxidized nicotinamide adenine dinucleotide; ADP, adenosine diphosphate; ATP, adenosine triphosphate; IMM, inner mitochondrial membrane; Q, ubiquinone; C, cytochrome c
Scheme made in part with images from https://smart.servier.com/

is still being investigated [45]. In the case of *Leishmania* in particular, the evidence suggests that complex I might be required only in some stages of its life cycle but this varies greatly from species to species [45].

Another peculiarity is the presence of alternative pathways that are absent in humans and other mammals. A well-known example of this is the alternative terminal oxidase of *T. brucei* that accepts electrons from reduced ubiquinone and reduces oxygen to water. This enzyme shares similarities with alternative oxidases found in higher plants, green algae and fungi [46].

In summary, all trypanosomatids exhibit an incredible repertoire of metabolic pathways, some unique to them, to facilitate their survival even in the most hostile and unlikely environments. Interestingly, there is no evident relationship between energy metabolism, phylogeny or even mode of transmission despite many of them being closely related and sharing the same habitats. This once again confirms the diversity and adaptability of these parasitic protozoans [28].

Coping with a hostile environment

While many pathogens actively avoid being internalized by macrophages or employ strategies to stop phagolysosome formation and flee to the cytosol, *Leishmania* is one of the few organisms known to thrive in such an adverse intracellular niche [47].

How this is accomplished is, up to this date, not well understood. Nonetheless, one key aspect for their survival inside macrophages is a successful differentiation from promastigotes to amastigotes.

During the differentiation process a number of metabolic changes take place: there's a decrease in the uptake and utilization of glucose, reduced organic acid secretion and increased fatty acid oxidation. The growth rate of the parasites also suffers a reduction. *In vivo* and *in vitro* differentiated amastigotes exhibit few differences in their metabolic profile. Still, the metabolism of amastigotes is an understudied issue when compared with promastigote metabolism, largely due to the difficulties in studying and culturing amastigotes [9,48].

The phagolysosome is predicted to have a wide range of carbon sources and micronutrients, since it's a compartment that receives several types of molecules not only via fusion with phagosomes, endosomes or autophagosomes, but also via transporters in the membrane of the phagolysosome. However, the levels of free sugars are considered to be quite low, and so, glucose is probably not the main carbon source for amastigotes. Indeed, amastigotes exhibit much lower rates of glucose uptake than promastigotes. Although *Leishmania* is capable of gluconeogenesis, it doesn't seem to be sufficient for survival in the absence of glucose [49,50]. Therefore, amastigotes also rely on amino acid catabolism and fatty acid β-oxidation as alternative carbon sources. Considering that the phagolysosome is a place for protein degradation, an abundance of amino acids is expected. Many pathways for the catabolism of amino acids, responsible for the generation of intermediates of the TCA cycle, have been identified. Moreover amino acids are also used by *Leishmania* as carbon skeletons for gluconeogenesis [29]. *Leishmania* can also degrade proteins in their own lysosome [50].

Fatty acids, obtained mainly from internalized lipoproteins, are also a major carbon source for *Leishmania*. Although trypanosomatids are unable to rely solely on fatty acids as an energy source due to the lack of the glyoxylate cycle (required for conversion of acetyl-CoA to hexoses), fatty acids probably have important roles in other biosynthetic pathways [30]. The acetyl-CoA produced through fatty acid oxidation enters the TCA cycle and ends up providing intermediaries for the biosynthesis of nonessential amino acids [50]. *Leishmania* amastigotes are also auxotrophic for a number of other nutrients like purines, vitamins and heme that they need to scavenge from the phagolysosome of the macrophage [50].

The intricate nutrient requirements of *Leishmania* could be the reason why these parasites, almost exclusively, infect macrophages and no other cell types. It is

possible that the phagolysosome of macrophages is the only compartment capable of sustaining amastigotes for long periods due to the great diversity of compounds that are delivered and processed. Nonetheless, this supposition needs further validation [47].

Such a complex energy metabolism ought to be tightly regulated, but surprisingly most genes are constitutively expressed along the life cycle of *Leishmania*, with only 5.7% of genes being down-regulated in amastigotes. This constitutive expression could be an adaptation to the fluctuations in nutrient availability in the hosts, facilitating a quick and effective response. As a result, the regulation of stage-specific changes must be done at the level of protein expression and/or post-translational modifications [30,51]. Hence, it is anticipated to find proteins that are only functional in certain stages of the parasite's life cycle.

One such example of a stage-specific protein is p27, a 27kDa subunit of the complex IV of the ETC that is only expressed in amastigotes. This protein was first characterized in *L. donovani* and it appears to be required for maximal activity of complex IV in amastigotes, considering that its absence decreases its activity and, consequently, ATP synthesis by oxidative phosphorylation [2]. Later studies showed that null mutants of the p27 had limited persistence and dissemination and were less virulent in mice. These results suggest a critical role for p27 during infection. Currently, $p27^{-/-}$ parasites of *L. donovani* and *L. major* are being studied to be used as a possible live attenuated vaccine [52–54].

The gene encoding p27 is located in chromosome 28 (*Leishmania* has a total of 36 chromosomes) and is highly conserved among several *Leishmania* species and to a lesser extent in some *Trypanosoma* species [2]. This gene is active and abundantly expressed in species that are both responsible for CL and VL, demonstrating the importance of p27 for the intracellular survival of the parasite regardless of the form of the disease that's occurring [55]. Nonetheless, the exact mechanism of action of p27 is still unknown.

Objectives

Leishmania infections can have severe impact on the hosts' health. Moreover, with limited treatment options it is crucial to understand the mechanisms that allow the parasite to survive and thrive in the vertebrate host. Mitochondrial function is believed to be a key factor at play, both in the initial and later stages of infection. It is also known that changes in protein expression occur when parasites differentiate from one stage to another and many of those are related with mitochondrial metabolism [32].

This work intends to shed some light on the complex mitochondrial function of *Leishmania infantum* (one of the causal agents of VL) and its relationship with infection in a mouse model. Accomplishing this will involve exploring further the relevance of p27 for complex IV function and its impact on parasite virulence. The aims above mentioned will be achieved by the creation of a collection of mutant strains of *L. infantum*: a null mutant of p27 ($p27^{-/-}$), a complemented strain ($p27^{-/-}$AB) and an overexpressing strain (p27OE). Each of these strains will be biochemically characterized and their ability to infect and survive in both macrophages and mice will be tested.

Materials and methods

Bioinformatics analysis

The gene encoding p27 (LinJ.28.1070) was obtained from the data base TriTrypDB (http://tritrypdb.org/tritrypdb/). Primers and scaffold needed to build gRNA and the template for the donor DNA (pTBlast plasmid) can be obtained from LeishGEdit (http://www.leishgedit.net/Home.html), an online resource for CRISPR-Cas9 genome editing in several kinetoplastids [56]. Mitochondrial targeting peptide prediction was done using the TargetP 1.1 Server (http://www.cbs.dtu.dk/services/TargetP/). Prediction of transmembrane domain was done using Phobius (http://phobius.sbc.su.se/).

To check the specificity of the primers sequences they were compared to sequences designed using the Eukaryotic Pathogen CRISPR guide RNA/DNA Design Tool (http://grna.ctegd.uga.edu/) with the following settings: SpCas9: gRNA length 20; PAM: NGG; off-target PAM: NAG, NGA. Using the BLAST tool in TriTrypDB these gRNAs were aligned with the rest of the genome of *L. infantum*. After this analysis, it was concluded that the gRNA sequences obtained from LeishGEdit were a good choice because they were specific to the p27 locus and presented the least homology with the remaining genome of *L. infantum*, thus minimizing the possibility of an off-target effect.

All the primers used throughout this work (table 1) were synthesized and purchased from Sigma-Aldrich and were diluted in the volumes indicated by the company to a final concentration of 20µM.

Table 1. Primers used throughout this work with the name assigned to each, respective sequence and brief description of their function. Underlined sequence is a T7 promotor. Sequences in **bold** are complementary to a region upstream or downstream of the p27 ORF and the sequence after it is complementary to the 3'-end of the gRNA scaffold. Sequences in blue represent homology flanks complementary to upstream or downstream regions of the p27 ORF. Restriction sites indicated in red; for primers P8 and P9 the restriction enzymes used were *Hind*III and *Kpn*I, respectively. Lowercase letters represent clamp sequences.

Name	Sequence (5'-3')	Description
P1	GAAATTAATACGACTCACTATAGG**ACAGCTCGCCTTGATCTA GT**GTTTTAGAGCTAGAAATAGC	Sense primer to build the 5'gRNA to ablate p27
P2	GAAATTAATACGACTCACTATAGG**ACGTGCAATCTTTAGGCG AG**GTTTTAGAGCTAGAAATAGC	Antisense primer to build the 3' gRNA to ablate p27
P3	AAAAGCACCGACTCGGTGCCACTTTTTCAAGTTGATAACGGA CTAGCCTTATTTTAACTTGCTATTTCTAGCTCTAAAAC	Scaffold to amplify synthetic gRNA

P4	GTGTGCGCGCACGTCCGCGCATTCAGTATAATGCAGACCTGCTGC	Sense primer to amplify the drug resistance cassette donor to ablate p27
P5	TGCGTGAAGGGGGAGGAGGGAGGGCCCAATTTGAGAGACCTGTGC	Antisense primer to amplify the drug resistance cassette donor to ablate p27
P6	CTTCGTCTGTTGGAGGAAGC	Sense primer to amplify drug resistance gene inserted in the p27 locus (for confirmation of successful ablation)
P7	CGAAGCACGCAACAAGAAGCA	Antisense primer to amplify drug resistance gene inserted in the p27 locus (for confirmation of successful ablation)
P8	cccaagcttATGTCTCGTTGCACGAACAAG	Sense primer to amplify p27 ORF from *L. infantum*
P9	gcgggtaccTTACACACCGTGGCCGGACAT	Antisense primer to amplify p27 ORF from *L. infantum*
P10	TGCTCTAGAGAAGCTGTGTCGGCGTGT	Antisense primer to confirm insertion of p27 into the pGL.TXN1 plasmid

Parasite culture

Leishmania infantum promastigotes (strain MHOM/MA/67/ITMAP-263) were cultured at 26°C in RPMI 1640 GlutaMAX™ medium (Gibco, Life Technologies™) supplemented with 20mM HEPES pH 7.4 (Sigma), 10% heat-inactivated FBS (FBSi; Gibco, Life Technologies™) and 50U/ml penicillin and 50µg/ml streptomycin (Gibco, Life Technologies™). Promastigotes expressing the plasmid pTB007 (Li-pTB007) were grown in the presence of 30µg/mL hygromycin B (Hyg, InvivoGen). The pTB007 is an expression plasmid for Cas9 and T7 RNA polymerase and is available on request at LeishGEdit.

Axenic amastigotes were differentiated from stationary phase promastigotes (5-7 days of growth). Briefly, promastigotes were counted (using a Neubauer chamber) and centrifuged at 3000rpm, 10min at room temperature. The supernatant was completely removed and the pellet was suspended in a small volume of MAA20. Approximately 1×10^7 parasites/mL were inoculated in 5mL of MAA20 medium in flasks with a filter cap at 37°C with 5%CO_2. The parasites were regularly monitored under the microscope and the medium was changed every 3-5 days (depending on the growth of the culture).

MAA consisted of medium 199 with Hanks' salts supplemented with 25mM HEPES, 4mM $NaHCO_3$, 14mM glucose and 0.5% soy trypto-casein broth (BioRad) to a

final pH of 5.8. This medium was filtered and stored at 4°C protected from light. When needed for culture this medium was supplemented with 0.023mM hemin (Sigma), 2mM Glutamax (Gibco) and 20% FBSi and sterilized by filtration once again (MAA20 medium).

To culture parasites collected from mice (see “Mice infections” and “Parasite burden determination” sections) complete Schneider’s medium was used. This medium consisted of Schneider’s insect medium (Sigma) prepared according to the manufacturer’s instructions and stored at 4°C protected from light. Before use, this medium was supplemented with 10% FBSi, 5µg ml^{-1} phenol-red (Sigma), 5mM HEPES and 100U ml^{-1} penicillin and 100µg ml^{-1} streptomycin.

PCR amplification of donor DNA

For amplification of the donor DNA, 10µL of Q5 Reaction Buffer 5x, 3% DMSO, 2µM of each primer (P4 and P5), 0.2mM dNTPs, 2µL of template (pT Blast, 30ng/µL [56]), 0.5µL Q5® High-Fidelity DNA Polymerase were mixed in 50µL total volume.

PCR steps were 5min at 94°C, 40 cycles of 30s at 94°C, 30s at 65°C, 2min 15s at 72°C and 7min at 72°C. From this reaction 2.5µL were analyzed in a 0.8% (w/v) agarose gel. The DNA was stored at -20°C until further use.

PCR amplification of gRNA

For amplification of the gRNA, two tubes were prepared with the following mixture: 10µL of Q5 Reaction Buffer 5×, 2µM of the primer P3, 0.2mM dNTPs, 0.5µL Q5® High-Fidelity DNA Polymerase. Then, to one of the tubes 2µM of the primer P1 and to the other the same concentration of the primer P2 were added in 50µL total volume in each tube.

The PCR steps were as follows: 5min at 98°C, 40 cycles of 30s at 98°C, 30s at 60°C, 15s at 72°C and 7min at 72°C. Amplified DNA was analyzed by agarose gel and was stored at -20°C.

Genomic DNA extraction

For the extraction of genomic DNA from *L. infantum* the Puregene Core Kit A (Qiagen) was used according to the following protocol: first, the culture (1-2mL) was centrifuged at 3000rpm, 10min. The pellet was washed in 200µL 1× PBS and centrifuged as before. The pellet was suspended in the residual volume left in the tube after discarding the SN. Then, 40µL of Cell Lysis Solution and 0.5µL of RNAse Solution (10mg/mL) were added. The tube was inverted several times and incubated 15min at 37°C.

The sample was then cooled at room temperature and 15µL of Protein Precipitation Solution was added and the mixture was vortexed for 20s. The tube was centrifuged at 14000rpm for 3min. The SN was transferred to a tube containing 0.8 volumes 100% isopropanol. The tube was inverted several times and centrifuged for 1min at 14000rpm. The pellet was washed with 70% (v/v) EtOH centrifuged once again and the supernatant removed. The pellet was left to dry at room temperature. After this, 15µL of DNA Hydration Solution was added and the sample was incubated for 1h at 65°C. The DNA was stored at 4°C.

PCR amplification and purification of p27

For amplification of the p27 ORF, 0.2 mM dNTPs, 0.56µM of each primer (820 and 821), 2% (v/v) DMSO, 0.5µL Q5® High-Fidelity DNA Polymerase (New England BioLabs Inc.), 10µL Q5 Reaction Buffer 5× (New England BioLabs Inc.) and 1.5µL template (*L. infantum* WT genomic DNA, 100ng/µL) in 50µL total volume. Twenty microliters of the same mixture (without template) was also prepared to serve as a negative control. PCR steps were 5 minutes at 95°C, 2 cycles of 30s at 95°C, 30s at 55°C, 40s at 72°C, 25 cycles of 30s at 95°C, 30s at 58°C, 40s at 72°C and 7 minutes at 72°C.

Following the PCR, 3µL of this reaction (mixed with 6µL of water and 1µL of 10× loading buffer) was run on a 0.8% (w/v) agarose gel to check for the presence of p27 ORF. After this confirmation, the DNA was desalted using the QIAEX II Protocol for Desalting and Concentrating DNA (Qiagen) and a new agarose gel was run (this time with 2 µL of DNA) to verify if there were no contaminants. The purified DNA was stored at -20°C

Construction of recombinant plasmids

To generate a strain over-expressing p27 (p27OE) and a complemented strain ($p27^{-/-}$AB), two plasmids were constructed and transfected into parasites. The backbone of the plasmids was the same, the only difference being the drug resistance gene, blasticidin for p27OE and hygromycin for $p27^{-/-}$AB.

A culture of *Escherichia coli* expressing the plasmid pGL.TXN1 was grown overnight in Luria broth media (LB) supplemented with ampicillin (100µg/mL). To extract the plasmid the GenElute™ Plasmid Miniprep Kit (Sigma) was used with some minor alterations: 10mL of culture were used (instead of 1-5 mL) and in the final step water was used instead of the Elution solution provided.

Three hundred nanograms of pGL.TXN1 plasmid were digested with 1µL of the restriction enzyme *Kpn*I (Thermo Fisher) and 2µL of *Hind*III (Thermo Fisher) and 5µL of 10× R buffer (Thermo Fisher) in a final volume of 50µL. The mixture was incubated over-night at 37°C. The p27 fragment (amplified in the previous section) was also digested in a similar manner but with 0.3µL of each restriction enzyme also in a final volume of 50µL.

An agarose gel was prepared to check for DNA digestion. After confirmation, the enzymes were inactivated at 80°C, 10min. A new 0.8% (w/v) agarose gel was run with the total volume of each mixture. The relevant bands were cut from the gel and processed according to the QIAEX II Agarose Gel Extraction Protocol (Qiagen) with some minor alterations: 7µL of QIAEX II beads was used instead of 10µL and digested p27 ORF and pGL.TXN1 were eluted in 25 and 40µL of water, respectively.

For the ligation of digested p27 with the plasmid, 26ng of p27, 24ng of pGL, 2µL of 10× T4 Ligase buffer (Thermo Fisher) and 1µL of T4 Ligase (Thermo Fisher) were mixed in a final volume of 20µL. For a control, another tube was prepared with everything except the insert but in a final volume of 10µL.

The recombinant plasmid (from now on designated pGL.BSD.p27) encoded a drug resistance gene for blasticidin, which is the same drug resistance as the $p27^{-/-}$ strain and, therefore, could not be transfected into these parasites. Hence, it was necessary to replace the BSD gene with a gene coding for a different drug resistance, and the one selected was hygromycin.

The gene encoding for hygromycin resistance was obtained from a pGL343 plasmid by digestion with *Spe*I and *BamH*I (0.5µL each) and 2µL of 10× Fast Digest Buffer (all from Thermo Fisher) in a final volume of 20µL for 1h at 37°C. The previously constructed plasmid pGL.BSD.p27 was digested in a similar way to remove the BSD

resistance gene. The ligation between the hygromycin insert and the plasmid was performed in an identical manner as described before. This new plasmid will be referred to as pGL.Hyg.p27.

Thus, two plasmids were prepared both contained the p27 ORF but different drug resistance genes. The fidelity of the p27 ORF was verified by Sanger sequencing (GATC Biotech: https://www.gatc-biotech.com/en/index.html). Both pGL.BSD.p27 and pGL.Hyg.p27 were stored at -20°C.

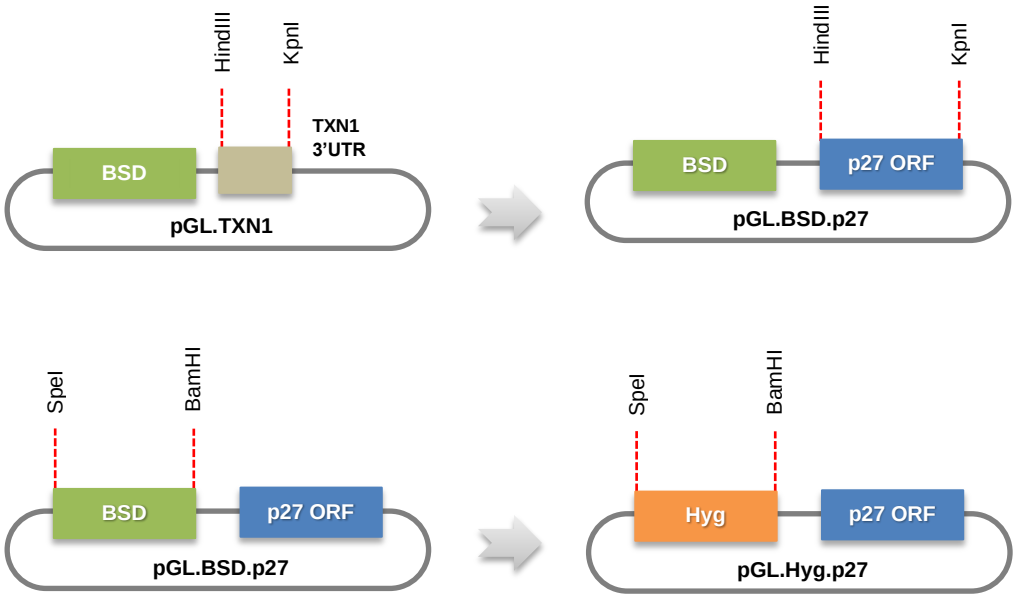

Figure 5. Schematic representation of the construction of the recombinant plasmids. Original pGL.TXN1 was digested with *Hind*III and *Kpn*I and p27 ORF fragment (digested with the same enzymes) was inserted into it, thus creating the pGL.BSD.p27 plasmid. The pGL.BSD.p27 was later digested with *Spe*I and *BamH*I to remove the gene encoding for blasticidin resistance (BSD) and insert the gene encoding for hygromycin resistance (Hyg), thus creating the pGL.Hyg.p27

Bacterial transformation

Three eppendorfs with 100µL of competent *E. coli* DH5α were defrosted. To each tube 10µL of pGL.BSD.p27 or pGL.Hyg.p27, empty pGL.TXN1 or water were added. The tubes with the empty plasmid and water were used as controls. The bacteria remained on ice for 30min. Next the tubes were placed in a bath at 42°C for 90s and then back on ice for 2min. Following this, 800µL of LB medium was added to each tube and these were incubated with agitation at 37°C for 1h.

Following incubation, 100µL of culture were plated into plaques containing LB medium and 50µg/mL ampicillin. The plates were incubated at 37°C over-night. Colonies were selected for PCR colony: 0.2µL DreamTaq Polymerase (Thermo

Fisher), 0.2mM dNTPs, 2% DMSO, 2µL 10× DreamTaq Buffer (Thermo Fisher), 1.2µL $MgCl_2$ (Thermo Fisher), 0.4µM of each primer (820 and 138), 20µL total volume. PCR steps were: 5min at 94°C, 30 cycles of 30s at 94°C, 30s at 53°C, 1:30min at 72°C and 7min at 72°C. The full PCR products were run on a 1% agarose gel to confirm the presence of p27 ORF in either the pGL.BSD.p27 or pGL.Hyg.p27 plasmids.

Positive colonies were selected and inoculated in 5mL of LB medium with 100µg/mL of ampicillin. The culture was let to grow over-night at 37°C with shaking. Plasmid DNA was extracted using the GenElute™ Plasmid Miniprep Kit. A 1% (w/v) agarose gel was run to confirm the presence of the plasmid. The fidelity of the cloned sequence was verified by Sanger sequencing as previously described.

DNA precipitation

DNA to be transfected into parasites was first precipitated in the following way: 3M sodium acetate pH 5.2 (1/10 of the volume of DNA) and 100% ethanol (2.5 times the volume) were added to the DNA in aqueous solution and the mixture was inverted several times and then incubated over night at -20°C.

The mixture was centrifuged at 14 000rpm for 30min at 4°C. The supernatant was discarded and, the pellet washed with 70% (v/v) ethanol and centrifuged once again for 5min in the same conditions as before. The supernatant was discarded and the pellet was air-dried for a few minutes in a flow chamber. A minimum of 5µg of DNA was used per transfection.

Parasite transfection

Logarithmic parasites (approximately 1×10^7 parasites/mL) were pelleted at 3000rpm for 10min, room temperature. The pellet was washed in Tb-BSF Buffer (90mM sodium phosphate, 5mM potassium chloride, 0.15mM calcium chloride and 50mM HEPES, pH 7.3) [57]. The DNA to be transfected (left to air-dry in the flow chamber) was suspended in 50µL of the same buffer. Two-hundred micro-liters of parasites were mixed with the DNA and transferred to a cuvette.

The Amaxa Nucleofector System was used with the program X-001. Next, the parasites were transferred to a culture flask with 10mL of RPMI medium. A control was prepared: culture flask with 10mL of the same medium and 200µL of non-transfected

parasites (mock). The cells were allowed to recover for 24h at 26°C. After this time, the cultures were diluted 1:5 and the respective selection drugs were added.

Li-ptB007 parasites [56] were transfected with the donor DNA and the 5' and 3'gRNA to ablate p27. WT parasites and $p27^{-/-}$ parasites were transfected with the pGL.BSD.p27 and pGL.Hyg.p27, respectively. The new strains, p27OE and $p27^{-/-}$AB were grown in 60µg/mL of blasticidin and 30µg/mL of hygromycin, respectively. Confirmation of $p27^{-/-}$AB and p27OE strains was performed by western blot.

Isolation of *Leishmania* $p27^{-/-}$ clones

Clones of $p27^{-/-}$ parasites were selected for clones by plating the polyclonal culture in agar plates containing blasticidin. The medium for the plates was prepared as follows: 1× M199 medium, 20% FBSi, 40mM HEPES, 50U ml^{-1} penicillin and 50µg ml^{-1} streptomycin, 0.1mM adenine and 0.007mM hemin and mixed with 1% agar (final concentration), previously autoclaved and cooled to ~50°C. For clone selection, blasticidin (30µg/mL) was added since it is the resistance coded by the donor DNA. Approximately 25mL of this solution was poured into plates and left to cool at room temperature until the agar was solid.

The polyclonal parasites were collected at 3000rpm, 10min. The supernatant was discarded and the cells were suspended in the residual medium left in the tube (roughly 100-200µL). The mixture was transferred to the plates and spread with a sterile glass spreader. The plates were briefly air dried and then wrapped in parafilm and incubated at 26°C.

Several days later, some colonies were collected and transferred to a 24-wells plate containing complete Schneider medium with 45µg/mL blasticidin and incubated at 26°C. When the parasites were sufficiently grown genomic DNA was extracted and PCR was performed. This was done by attempting to amplify the p27 ORF (using primers P8 and P9) and amplification of the drug resistance gene in the p27 locus using primers P6 and P7. A western blot was also performed using α-p27 antibody.

Confirmation of ablation of p27 was done by PCR amplification of p27 ORF and blasticidin resistance ORF and western blot (antibody α-p27).

Mice infections

Female (n=12) and male (n=14) C57/BL6 mice (all around 6 weeks old) from the i3S Animal Facility were used in the experiments. The animals were housed in same-sex groups (2-5 individuals per cage) at 22-24°C and had a 12-12h light/dark cycle. They had *ad libitum* access to water and food in the form of pellets.

Mice were restrained and injected intravenous in the tail vein with 2×10^7 stationary-phase WT or $p27^{-/-}$ parasites using a 26G needle. The animals were euthanized at 7, 21 and 56 days post-infection by isoflurane overdose followed by cervical dislocation (as a confirmation of death).

The spleen and liver were removed, weighted and placed inside $10cm^3$ glass mortar tubes with complete Schneider's medium (2mL of medium for the spleens and 3mL for the livers). All this work was conducted in a flow chamber in an ABSL2 room of the animal facility. A minimum of four animals per strain per time-point was used and male and female animals were infected with both strains.

Parasite burden determination

The spleen and liver inside the glass mortar tubes were homogenized using sterile piston-type Teflon® pestles (one per tube) that were attached to a stirrer motor. The lower speed settings were used. The volume of the suspensions was determined and transferred to falcon tubes.

The concentration of the suspension was calculated and diluted in complete Schneider's medium to a final concentration of 10mg/mL in a final volume of 2mL for the spleens and 5mL for the livers. Two-hundred microliters of this suspension of organs was transferred to the first column of 96 well plates and then serial dilutions of 1:4 in quadruplicate were made. Each plate contained the suspensions of liver and spleen from one animal (figure 6).

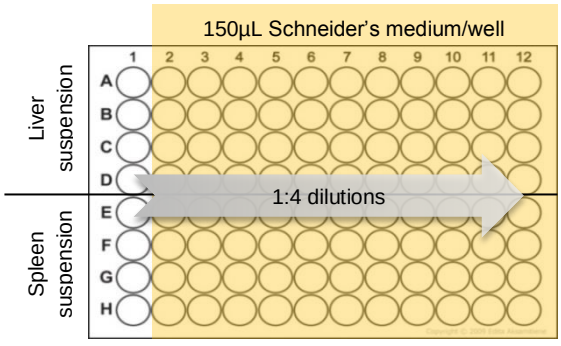

Figure 6. Schematic representation of the organization of the plates. Column1 lines A-D contained 200µL of liver suspension and lines E-F contained 200µL of spleen suspension. Concentration of both suspensions was 10mg/mL.

The plates were sealed with parafilm and incubated at 26°C. After 15 days of incubation the number of positive wells (presence of parasites) was determined by inverted microscope observation.

Macrophage infection

Bone marrow derived macrophages (BMDM) were obtained from C57/BL6 mice (protocol adapted from [58]) and were cultured in 96 wells plates in Dulbecco's Modified Eagle's Medium (DMEM) completed with 10% FBSi, 1% (v/v) Minimum Essential Medium Non-Essential (MEM) amino acids solution and 50U/ml penicillin and 50µg/ml streptomycin (all from Gibco, Life Technologies™) plus 15% (v/v) L929 cell conditioned medium (LCCM).

BMDM were infected with stationary phase parasites (8 days of growth) at 20:1 ratio (parasites:macrophages). After 3h of incubation at 37°C and 5% CO_2 the cells were washed 2-3 times with cDMEM (without LCCM) to remove non-internalized parasites. After washing, the plates were re-incubated in the same conditions for 24, 48, 72 and 96 hours in cDMEM medium supplemented with 5% (v/v) LCCM.

At the end of each time-point the medium was removed and 30µL of 4% (w/v) paraformaldehyde in 1×PBS was added to each well and incubated at room temperature for 15 minutes. Then the cells were washed twice with 1×PBS. Next, 30µL of 0.1% (w/v) Triton X-100 (Sigma) in 1×PBS were added and incubated at room temperature for 15 minutes.

Plates were washed twice with 1×PBS and to each well 30µL of a solution containing 0.75µL HCS CellMask™ Deep Red stain (10mg/mL, Invitrogen) in 10mL of DAPI (5mg/mL) was added and incubated for 45 minutes at RT. After washing as before, 50µL of 1× PBS was distributed to each well.

Reading of the plates was performed in the IN Cell Analyzer 2000 microscope (GE Life Sciences) and the results were analyzed using the IN Cell Developer Toolbox 1.9.2 software with the settings described by Gomes-Alves *et al.* [59].

Western blot

Parasites were counted, centrifuged (3000rpm, 10min, RT) and washed twice in 1×PBS. The pellet was resuspended in the residual volume of PBS and the cells were

lysed with a solution of 4% (w/v) SDS in 50mM Tris-HCl pH 7.6 (8µL per 5×10^6 parasites). The samples were vortexed and frozen at -20°C until further processing.

Ten microliters of sample were mixed with 10µL of 1×PBS and 5µL of loading buffer (250mM Tris-HCl pH 6.8, 10% (w/v) SDS, 0.5% bromophenol blue, 50% glycerol) which were then vortexed and incubated for 10 minutes at 65ºC. Twenty microliters of this mixture was loaded into the wells of a 12% SDS-PAGE gel and the gel was run at 25mA. Next, the proteins were transferred to a nitrocellulose Hybond-C Extra membrane (GE Biosciences).

The membrane was stained with Ponceau S to ascertain the quality of the samples, transference and also to allow the visualization of the molecular weight marker. Ponceau S removal was achieved by a serial of washes with dH_2O, transfer buffer (25mM Tris, 192mM glycine and 20% (v/v) methanol), dH_2O again and finally with 1×TBS-T (20mM Tris-HCl, 137mM NaCl, 0.1% Tween 20, pH 7.6). The membrane was blocked with 5% (w/v) milk in TBS-T for at least 1h.

Afterwards, the milk was removed, the primary antibody was added and left to incubate over-night with agitation at 4°C. The membrane was washed 3 times for 15 minutes with 1×TBS-T followed by incubation with the secondary antibody for 1-2h. After another washing cycle like afore mentioned, the membrane was revealed using Clarity™ western ECL substrate (BioRad) chemiluminescence kit. The images were acquired at the ChemiDoc XRS+ (BioRad) using the software ImageLab.

Table 2 contains the antibodies used throughout this work and their respective dilutions. The antibody against p27 was gently offered by Dr. Robert Duncan of the Division of Emerging and Transfusion Transmitted Diseases, Center for Biologics Evaluation and Research, FDA, Bethsda, MD, USA.

Table 2. List of antibodies used in the western blots performed throughout this work. Values inside parenthesis indicate the dilution used.

Primary antibody	Secondary antibody
α-p27 (1:2 000) α-mTXNPx (1:2 000) α-COXIV (1:2 000)	α-rabbit (1:10 000)

Blue native polyacrylamide gel electrophoresis (BN-PAGE)

Logarithmic parasite cultures were counted and centrifuged at 3000rpm, 10min RT. The pellet was washed once in 1×PBS and the supernatant was completely

removed. For 1×10^8 parasites the pellet was suspended in 500µL of 1xSoTE (20mM Tris/HCl pH 7.4, 0.6M sorbitol and 2mM EDTA) and then in 500µL of 0.06% (w/v) digitonin (DIG) in 1x SoTE solution. The tubes were gently inverted 3-5x and incubated on ice for 5min. Next, samples were centrifuged at 8000rpm, 4°C, 5min and the pellet was washed (without resuspending) in 1x SoTE solution. Samples were centrifuged again as described previously.

The pellet was carefully ressuspended in 130µL solubilization solution (55.55mM NaCl, 55.55mM imidazole pH 7, 11.11% (w/v) glycerol, 5.55mM aminocaproic acid and 1mM EDTA) plus 4g DDM/g protein. This mixture was incubated on ice 30min with frequent vortexing. Following this, the mixture was centrifuged at maximum speed, 30min at 4°C and the supernatant was transferred to new tubes.

BN-PAGE gels were mounted as described in table 3. Twenty-five microliters of the supernatant were loaded onto each well. Composition of cathode buffer was: 50mM tricine, 7.5mM imidazole pH 7.0, 0.02% Coomassie Blue G250. Anode buffer consisted of 75mM imidazole pH 7.0. The gel was run over-night at 50V at 5-6°C.

Table 3. Composition of the 7% non-gradient separation gel and the 4% sample gel used to isolate complex IV of the respiratory chain

	7% separation gel	4% sample gel
A-B mix (30% acrilamide, 1.125% bis acrilamide)	2.334 mL	0.4 mL
Gel buffer 3x (75mM imidazole, 1.5M aminocaproic acid, pH 7)	3.334 mL	1 mL
Glycerol 85%	0.91g	-
dH_2O	3.552 mL	1.6 mL
10% APS	50µL	25µL
TEMED (Sigma)	5µL	2.5µL
Final volume	10 mL	3 mL

At the end of the run, part of the gel was used for COX in-gel activity assays and the rest was transferred to a PVDF membrane to perform a western blot. For the in-gel activity assay the gel was washed in a solution of 50mM sodium phosphate pH 7.4 for 15-20 minutes and then incubated in 12.5mL of a solution of 50mM Sodium phosphate, 7.5mg 3, 3-diaminobenzidine (DAB) tetrahydrochloride and 7.5mg cytochrome c from horse heart (Sigma) for several hours in the dark. Relative

quantification of band intensity was performed on the image processing package Fiji [60].

The transfer was performed in a semi-dry system. First, the gel was incubated in transfer buffer with 0.1% SDS for 15min at RT. The PVDF membrane was activated by dipping it in pure methanol. The membrane and the filter paper were dipped in transfer buffer and placed in the system. A heavy object was placed on the lid (>1kg). The proteins were transferred for 2h at 150mA.

At the end, the blue color of the membrane was removed by incubating it with agitation in a solution of 62.5mM Tris pH 6.7, 2% (w/v) SDS, 0.1M β-mercapto-ethanol during 15-30min with 2-3 substitutions of the solution. The membrane was then washed 3 times with dH_2O and once in 1×TBS-T. From this point, the procedures (blocking, incubation, revealing, etc.) were the same as described in the section "Western blot".

Oxygen consumption

Parasite culture of either logarithmic promastigotes or 3 days old amastigotes were counted and centrifuged at 3000rpm, 10min RT, washed once in 1×PBS and suspended to a final concentration of 3×10^8 parasites/mL in 1×PBS. Oxygen consumption was constantly measured in a sealed incubation chamber at room temperature using a Clark-type oxygen electrode (Hansatech).

The following solution was prepared and loaded into the chamber: 0.3M sucrose, 10mM potassium phosphate pH 7.2, 5mM $MgCl_2$, 1mM EGTA, 10mM KCl, 4µM CCCP, 0.02% (w/v) BSA and 3×10^7 parasites. After measuring basal oxygen consumption in promastigotes, 1mM KCN was added to inhibit complex IV, thus, halting oxygen consumption [61].

Assays with amastigotes were conducted using the previous solution. Basal oxygen consumption was measured and complex III was inhibited by the addition of 0.2µg/mL antimycin A followed by 2.5µL 1% DIG to permeabilize the amastigotes without killing them. After stabilization of the signal, 5mM of sodium L-ascorbate (Sigma) and 0.5mM TMPD (Sigma) were added. All the results were analyzed using the O2view software version 1.02 (Hansatech).

Statistical analysis

Statistical analysis of differences between groups was determined by two-way ANOVA using GraphPad Prism version 5.0 for Windows, GraphPad Software, San Diego California USA (https://www.graphpad.com/).

Results

In silico analysis

Initially, we attempted to list all subunits of cytochrome c oxidase (COX) of *Leishmania infantum* and compare them with the subunits of a related protozoan (*Trypanosoma brucei*) and a mammal (*Mus musculus*). Protein sequences of the subunits of COX are described in the databases TritrypDB and UniProt (https://www.uniprot.org/).

Eleven subunits were uncovered with a total molecular weight of 301 723 Da (assuming the enzyme is composed by a single polypeptide of each protein). Although *L. infantum* and *T. brucei* subunits share a relatively high percentage of homology, no such homology was found when comparing these sequences to the ones of *M. musculus* (table 4). In fact, either the trypanosomatid COX proteins have no identified counterparts in mammals or they diverged in during evolution and homology is no longer detected.

Table 4. Subunits of complex IV of the respiratory chain in three different organisms. Abbreviations: MW, molecular weight; ID, gene code; Da, Dalton; cyt c, cytochrome c; e^-, electrons; N/A, not applicable; ***** mitochondrial encoded subunits in *L. infantum* not found in TritrypBD. Values for MW refer to *T. brucei* and ID is from UniProt; **†** mitochondrial encoded subunit not found in either TritrypBD or Uniprot. ID refers to GenBank.

Leishmania infantum			***Trypanosoma brucei***	**% Identity**
ID (TritrypDB)	**Protein name**	**MW (Da)**	**ID (TritrypDB)**	
N/A	Cytochrome c oxidase subunit 1 *****	63 348	**P04371**	N/A
N/A	Cytochrome c oxidase subunit 2 *****	24 220	**P04372**	N/A
N/A	Cytochrome c oxidase subunit 3 **†**	39 690	**AAA32122.1**	N/A
LinJ.12.0620	Cytochrome oxidase subunit IV	39 596	**Tb927.1.4100**	76
LinJ.26.1690	Cytochrome c oxidase subunit V	22 282	**Tb927.9.3170**	87
LinJ.21.2080	Cytochrome c oxidase subunit VI	19 225	**Tb927.10.280**	85
LinJ.25.1170	Cytochrome oxidase subunit VII	19 055	**Tb927.3.1410**	72
LinJ.31.1600	Cytochrome c oxidase subunit VIII	18 811	**Tb927.4.4620**	71
LinJ.36.7350	Cytochrome oxidase subunit IX	13 749	**Tb927.10.8320**	81
LinJ.23.0420	Cytochrome c oxidase subunit X	14 114	**Tb927.11.13125** **Tb927.11.13140**	74
LinJ.28.1070	p27 protein	27 633	**Tb11.0400**	67

Mus musculus		
ID (UniProt)	**Protein name**	**Function**
P00397	Cytochrome c oxidase subunit 1	Catalytic subunit
P00405	Cytochrome c oxidase subunit 2	Transfers e^- from cyt c to subunit 1
P00416	Cytochrome c subunit 3	Part of the functional core
P19783	Cytochrome c oxidase subunit 4 isoform 1	

Q91W29	Cytochrome c oxidase subunit 4 isoform 2	
P12787	Cytochrome c oxidase subunit 5A	
P19536	Cytochrome c oxidase subunit 5B	
P43024	Cytochrome c oxidase subunit 6A1	Essentially involved in the regulation of oxygen consumption and proton translocation by Complex IV
P43023	Cytochrome c oxidase subunit 6A2	
P56391	Cytochrome c oxidase subunit 6B1	
Q80ZN9	Cytochrome c oxidase subunit 6B2	
Q9CPQ1	Cytochrome c oxidase subunit 6C	
P56392	Cytochrome c oxidase subunit 7A1	
P48771	Cytochrome c oxidase subunit 7A2	
P17665	Cytochrome c oxidase subunit 7C	
Q64445	Cytochrome c oxidase subunit 8A	
P48772	Cytochrome c oxidase subunit 8B	
A6H666	Cytochrome c oxidase subunit 8C	

One of the COX subunits, protein p27, is stage-specific being only expressed in amastigotes. It has a molecular weight of 27633 Da, composed by 240 amino acids and it has one predicted transmembrane domain [2]. The sequence is highly conserved among *Leishmania* species and less conserved in other trypanosomastids but the exact function of this protein remains unknown.

While doing a BLAST analysis of p27 against the whole genome of *L. infantum*, a similar hypothetical protein (also of unknown function) was encountered. This protein (we'll call it p28 for simplicity) shares 63% identity with p27 (72% homology at the gene level) and it's 27843 Da and composed by 243 amino acids (figure 7). It also has one predicted transmembrane domain and a putative mitochondrial targeting peptide is predicted.

```
p27   1    MSRCTNKISGGTARANLVDHGVYVKPMSLNPFLGAVHDGTSTGYCQGYSAKPMHWLYRFR  60
           MSR +NKISGG A   ++DHG Y+KPM+ NP+L   HDG +T Y QG++ K  HWLYRFR
p28   1    MSRVSNKISGGRACQTVIDHGYYLKPMTGNPYLCTQHDGVTTAYQQGFAPKDAHWLYRFR  60

p27   61   YNVLPQGISCGFFSRNPYGRYVHWLEVSTIEKIRMQLQSVESMPVSVLVTLVVIYSLWFS  120
           YN+LPQG+S GFFSRNPYGRYVHWLEVSTIEK+R+Q+ ++ES+P SV+  +++++++W S
p28   61   YNLLPQGMSGGFFSRNPYGRYVHWLEVSTIEKMRLQMLTMESVPCSVVSVILLVFTMWHS  120

p27   121  YRLTFLHPDITLYNLGLWSTKPWVQQQRFNKKIDIDQQVYRWVHRVPEFSITDPIREIYK  180
           YRL FLHPDITLYNLGLW TKPWVQQQRFNKK + DQ VYRWV R PEF I DPIR++YK
p28   121  YRLAFLHPDITLYNLGLWPTKPWVQQQRFNKKKEFDQDVYRWVCRAPEFMIDDPIRDMYK  180

p27   181  LEIGANEPYLEHVRGMGREKELTLYANERTEGAGSIR  217
           + I AN+P L   +  G   ++T+   E T  A  IR
p28   181  MGIAANDPVLAMAKEQGVASQMTMAQAEYTSAAPDIR  217
```

Figure 7. Alignment of p27 and p28. This analysis was performed using the BLAST tool in the database TriTrypDB. Blue rectangles represent transmembrane domains.

Despite the similarities between p28 and p27, the first was never identified as a subunit of COX, nonetheless the information about this protein is still scarce. The sequence is also conserved among *Leishmania* species and to a lesser extent in other trypanosomastids.

p27 ablation

An *L. infantum* p27 null mutant was generated using the CRISPR-Cas9 method. First, an expression plasmid for Cas9 and T7 RNA Polymerase (pTB007) was obtained from LeishGEdit [56] and transfect into WT parasites. Constitutive expression of Cas9 had no apparent negative effects on *L. infantum* promastigotes. These parasites showed normal growth rates and morphology. Primer sequences to build gRNA and the donor cassette (pTBlast) with the blasticidin resistance gene (BSD) were also obtained from LeishGEdit. The 5' and 3' gRNA templates and the donor cassette were produced by PCR (figure 8a and 8b) and the resulting products were transfected simultaneously into parasites expressing pTB007.

The polyclonal culture was plated and several clones were selected. Identification of knockout parasites was initially done by PCR amplification of the p27 ORF using primers P8 and P9 (figure 8c and 9a). This allowed the immediate exclusion of parasites containing the p27 ORF. Following this, we analyzed the apparently positive clones and amplified the BSD ORF in the p27 locus using primers P6 and P7.

Primer P6 anneals 200bp upstream of the p27 ORF and primer P7 anneals 200bp downstream (figure 8c). So, the expected size of the band for WT parasites should be 1.1kb, for double knock-out 2.1kb (the donor cassette alone has 1.7kb) and single knock-out parasites should have two bands, one of each size.

Of the selected clones, only one (number 19) seems to be a single knockout, although the 1.1kb band is very faint and could also be the result of a small contamination (figure 9b). The remaining parasites were double knockouts for p27 ORF with a successful insertion of the drug resistance cassette in both alleles. Even the polyclonal culture seemed to be composed of only double knockouts (figure 8c and 9b).

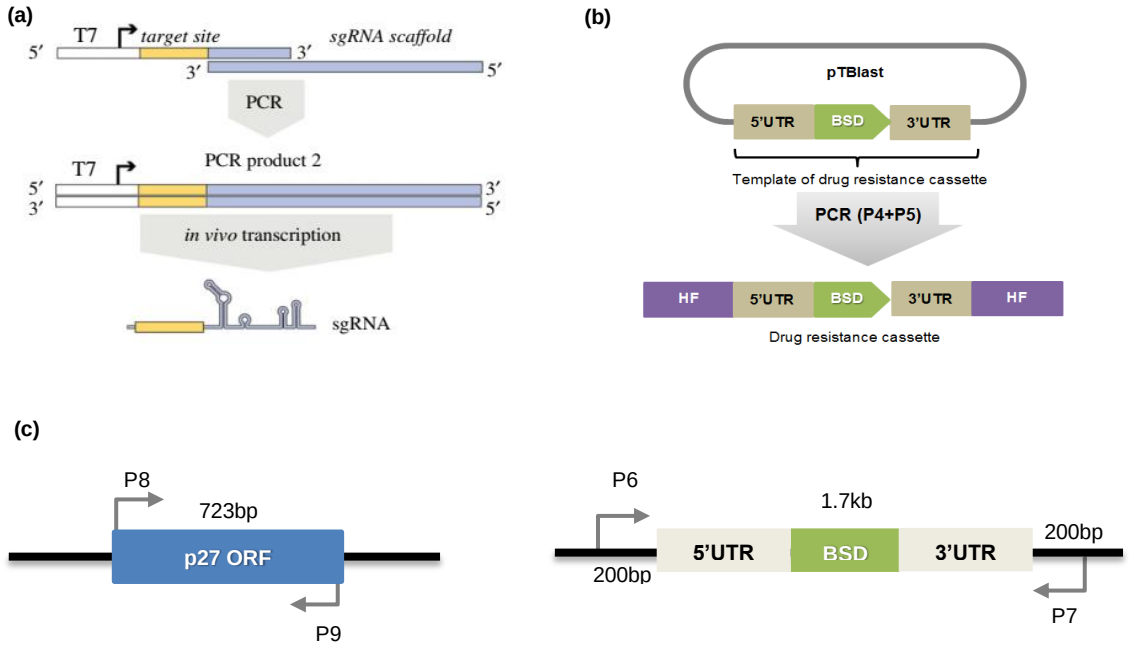

Figure 8. CRISPR-Cas9 strategy for ablating p27. **(a)** Generation of the gRNA templates by PCR. Scheme adapted from [56]. **(b)** Generation of the drug resistance cassette obtained from pTBlast plasmid. **(c)** p27 locus before (left) and after (right) CRISPR-Cas9 ablation. Primers are identified by the letter "P" followed by a number as well as their respective positions of annealing. Primers are described in the section "Bioinformatics analysis" of "Materials and methods". HF indicates homology flanks. These are sequences homologous to regions upstream or downstream of the ORF that allow the insertion of the drug resistance cassette by homologous recombination.

Clone 20 was selected to perform all the following experiments in this work and these parasites will be referred to as p27$^{-/-}$ from now on. Promastigotes lacking the p27 ORF showed neither an impaired growth rate (figure 10) nor morphological abnormalities. The p27$^{-/-}$ parasite culture was indistinguishable from WT parasites. These parasites were also able to be converted into morphologically normal amastigotes although the culture density was almost always lower than a WT culture.

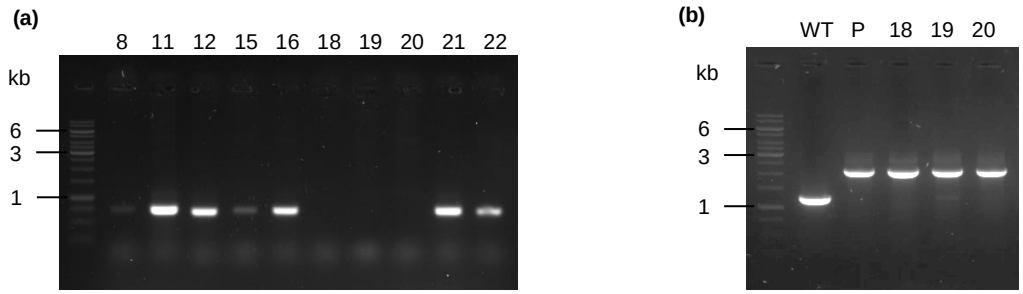

Figure 9. PCR confirmation of p27 ablation. Numbers on top of the images indicate different clones. P = polyclonal culture. Numbers on the left indicate the molecular weight in kilobases (kb). **(a)** Agarose gel showing the absence of p27 ORF in three clones (18, 19 and 20); primers used were P8 and P9. **(b)** Agarose gel showing the results of a PCR used to test if the insertion of the BSD ORF in the p27 locus was successful. Primers used were P6 and P7

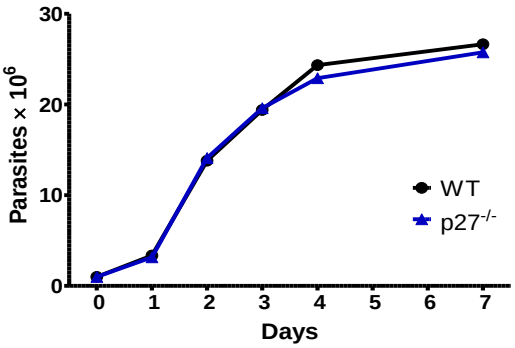

Figure 10. Growth curve of WT and p27$^{-/-}$ promastigotes. 1×10^{6} parasites were inoculated in 5mL of RPMI and counted every day for 7 days

Generation of p27OE and p27$^{-/-}$AB strains

The expression of p27 was restored in an add-back strain by transfecting p27$^{-/-}$ parasites with the pGL.Hyg.p27 plasmid (p27$^{-/-}$AB). An over-expressing strain (p27OE) was also created by transfecting WT parasites with the pGL.BSD.p27 plasmid. Confirmation of p27 protein expression from these recombinant episomes was done by western blot using an antibody against p27 (figure 11).

Like the p27$^{-/-}$ promastigotes, these new strains showed no differences in growth rate or morphology when compared to WT. These parasites were also converted into morphologically normal amastigotes and had a culture density very similar to WT.

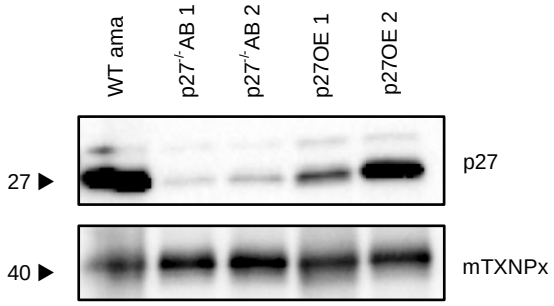

Figure 11. Western blot confirming p27 expression in the different strains. WT amastigotes with 3 days of growth (WT ama) were used as a positive control for p27 expression. The remaining samples were taken from logarithmic promastigotes grown with two different drug concentrations: p27$^{-/-}$AB 1 - 20µg/mL; p27$^{-/-}$AB 2 - 30µg/mL; p27OE 1 - 30µg/mL; p27OE 2 - 60µg/mL. mTXNPx was used as a loading control

p27 expression along parasite differentiation

It is known from studies in other *Leishmania* species that the protein p27 is only expressed in amastigotes [2]. Here we investigate exactly when does this protein starts

to be expressed in *L. infantum* parasites. Therefore, samples from parasites along different time-points in the differentiation process were collected and analyzed by western blot. In the first 12h hours after inoculating stationary promastigotes in MAA20 and incubating them at 37°C 5% CO_2 there was no expression of p27 (data not shown). p27 starts to be expressed after 24h and increased progressively along time (figure 12). By 72h after inoculation, the levels of expression were similar to an established culture of axenic amastigotes. At 96h there was an apparent decrease in the expression, which was probably due to the aggregation and/or death of parasites.

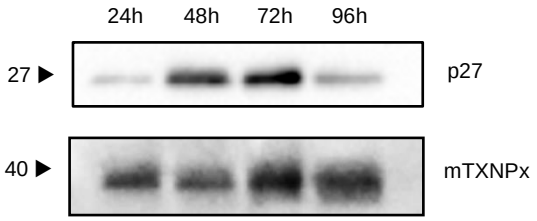

Figure 12. p27 expression along the differentiation of promastigotes into amastigotes. Numbers on the left indicate the molecular weight in kDa. mTXNPx was used as a loading control

p27 expression trigger

It is believed that a decrease in pH and an increase in temperature are the factors responsible for amastigote differentiation. We decided to investigate which, if not both, of these two stimuli contributed more to the expression of the p27 protein. To accomplish this, parasites were cultured in four different conditions: 1) RPMI, pH~7 at 26°C (normal medium for promastigotes); 2) MAA20, pH~5 at 37°C (normal medium for amastigotes); 3) RPMI, pH~7 at 37°C; 4) MAA20, pH~5 at 26°C. All the cultures were incubated for approximately 3 days. Protein extracts from the different samples were then analyzed by western blot.

As shown in figure 13, p27 is highly induced upon incubation of promastigotes in amastigote differentiation conditions (MAA20, 37°C). Furthermore, temperature seems to be a more critical stimulus for p27 expression than pH because of a higher expression of p27 in WT parasites when placed in RPMI at 37°C than in MAA20 at 26°C is observed. However, this level of expression is very low when compared with WT amastigotes, suggesting that the two stimuli are necessary for the full expression of the protein.

We also analyzed the expression of another subunit of complex IV, COXIV, under the same conditions, and found that COXIV expression is constant, regardless of the condition and strain tested. These results indicate that ablation or overexpression of p27 does not impact the expression of other complex IV subunits.

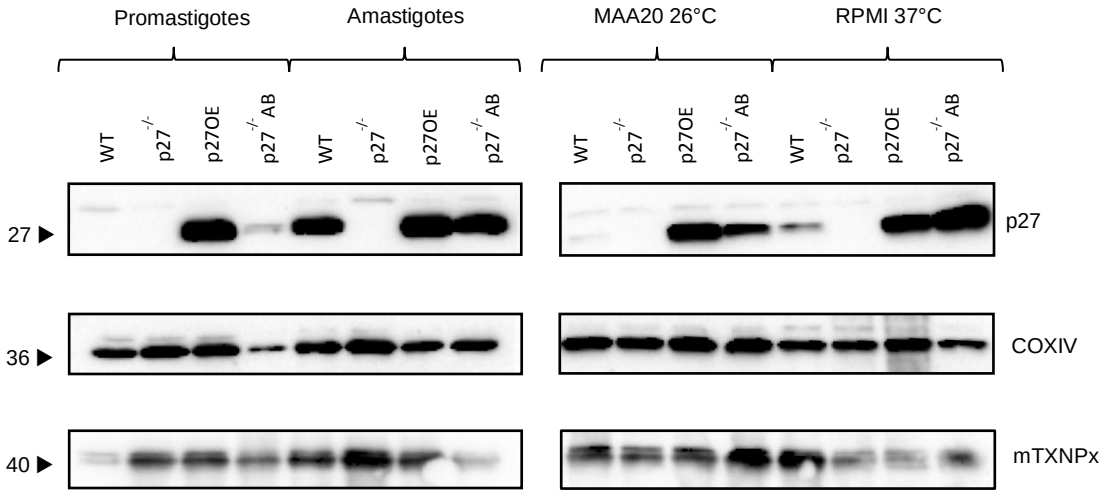

Figure 13. Impact of pH and temperature on the expression of two subunits of complex IV in different conditions. Numbers on the left indicate the molecular weight in kDa. The proteins detected are identified on the right. The protein mTXNPx was used as a loading control

Infection of BMDM

Since we found no significant changes in morphology, growth rate or complex IV expression between the different strains, we decided to test the capability of these parasites to infect and survive in macrophages. BMDM from C57/BL6 mice were infected with stationary phase promastigotes of the four strains: WT, $p27^{-/-}$, p27OE and $p27^{-/-}$AB.

All strains infected macrophages at similar rates in the first 24h. Nevertheless, while WT, $p27^{-/-}$, $p27^{-/-}$AB remained with very similar values and all showed a downward trend in the percentage of infection, p27OE showed significantly higher infection values (left graph, figure 14). In fact, p27OE appears to have a significantly higher infective capacity (right graph, figure 14), their intracellular numbers from 24h to 72h seeming to be increasing, while the other strains displayed a slight reduction in the number of parasites per cell throughout time.

In summary, the absence of p27 is indifferent in regards to the outcome of infection in BMDM, although when the protein is over-expressed (p27OE strain) the

parasites appear to be more virulent. Nonetheless it is important to notice that the variability of these experiments is high.

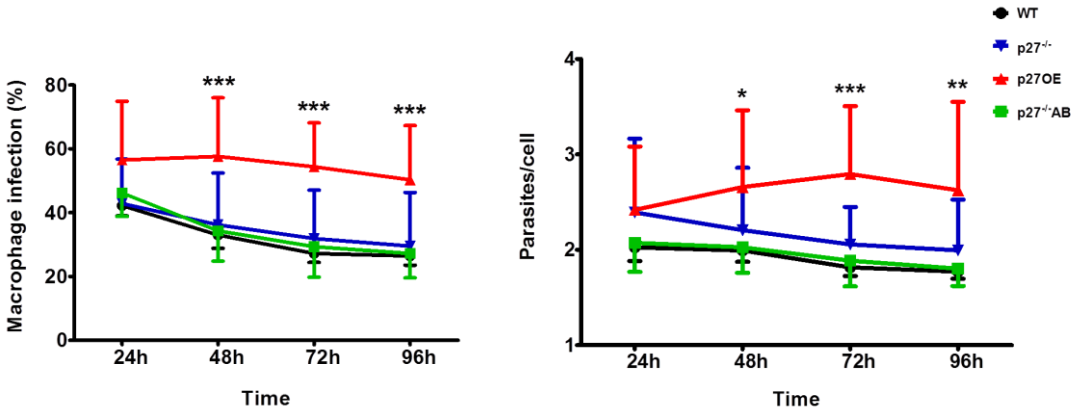

Figure 14. BMDM infected with WT, p27$^{-/-}$, p27OE and p27$^{-/-}$AB were cultured for the indicated time. Infection efficiency (percentage of infection, left) and intracellular growth (parasites/cell, right) are represented in the graphs. Results are shown as the mean of three different experiments (each of them in triplicates) and SEM (standard error of the mean). Statistical differences are in relation to WT.

* P<0.05; ** P<0.01; *** P<0.001

In vivo infection

Since the p27$^{-/-}$ parasites ability to infect macrophages was not impaired and p27OE parasites proved to be the most virulent strain, it was tantalizing to see how all of these strains would behave in a vertebrate host. Yet, only the WT and p27$^{-/-}$ were used in the *in vivo* experiments, since the p27OE and p27$^{-/-}$AB strains were not created in time to be included.

C57/BL6 mice were infected intravenously with 2×10^7 parasites. Parasite burden was determined by serial dilution at 7, 21 and 56 days post-infection (p.i.). WT parasites exhibited the expected behavior in the liver and spleen. In the spleen the parasite burden was lower than in the liver but fairly constant from 21 days p.i. onwards. In the liver there was a peak at 21 days p.i. and then a considerable decrease.

The p27$^{-/-}$ parasites exhibited a very different behavior, although they were able to infect both the liver and spleen. In the spleen, the parasite burden decreased throughout time being always very low except in the first time-point where values are similar to the WT. In the liver the parasite burden is significantly lower than in mice infected with WT parasites in each time-point. Moreover, no peak of infection is observed in the liver of p27$^{-/-}$ infected mice where parasites seem to have a tendency

to be completely cleared (figure 15). Overall, p27$^{-/-}$ parasites are not able to proliferate neither in the spleen nor in the liver of C57/BL6 mice.

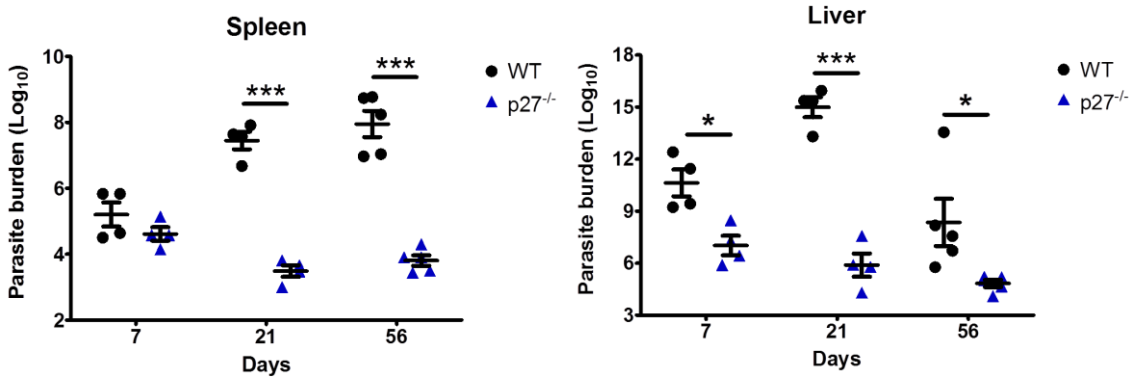

Figure 15. Parasite burden in the spleen and liver of C57/BL6 mice infected with WT or p27$^{-/-}$ stationary promastigotes at 7, 21 and 56 days post-infection. Results are represented as mean ± SEM and each black dot or blue triangle represents a different animal.
* P<0.05; *** P<0.001

Complex IV activity and p27

The *in vivo* results revealed the impact that the loss of p27 has on parasite virulence and to explore this issue we decided to determine the activity of complex IV in all the strains, since a reduced ability to produce energy could explain the parasite's inability to proliferate and survive in the host.

For that crude mitochondrial extracts from the four strains were solubilized with a non-ionic detergent and resolved in a native gel. Coomassie staining of the gel revealed that all the samples contained roughly the same amount of protein (figure 16a). Furthermore, COX in-gel activity assay (figure 16b) led to the detection of a band at approximately 800kDa that corresponded to complex IV.

The activity staining revealed that WT parasites had the lowest band intensity and p27$^{-/-}$ and p27$^{-/-}$AB, the highest values, the latter being the one with the most intense band (table 6 and figure 16b). Besides the expect band corresponding to the activity of complex IV, two other bands of approximately 440kDa appeared in all strains but with higher intensity in p27$^{-/-}$ and p27$^{-/-}$AB. These bands could represent complex IV assembly intermediates with activity.

A western blot analysis (figure 16c), using an antibody against p27, confirmed the association of p27 with complex IV in WT and p27OE strains and the complete absence of p27 in the null mutant. The p27$^{-/-}$AB parasites although able to express p27, as shown previously, did not have it associated to complex IV in this experiment. As for

the in-gel activity, a lower molecular weight band of 440kDa is detected by the α-p27 antibody. This band is more intense in p27OE and p27$^{-/-}$AB, fainter in WT and not visible in p27$^{-/-}$. Summarizing, complex IV appears to be functional and more active in the absence of p27.

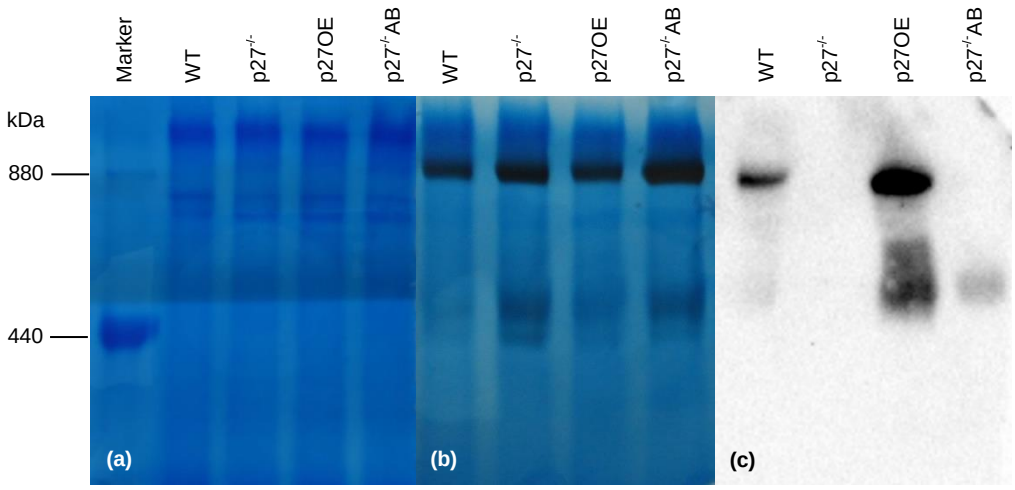

Figure 16. BN-PAGE analysis of crude mitochondrial extracts from WT, p27$^{-/-}$, p27OE and p27$^{-/-}$AB amastigotes. **(a)** Coomassie staining with ferritin (10μg/10μL) marker in the left lane. **(b)** COX in-gel activity. **(c)** Western blot analysis. The antibody α-p27 was used to confirm the association of p27 with complex IV.

Table 5. Quantification of intensity in the COX in-gel activity assay (figure 16b). Values are represented as the net band value over the net loading control (in this case the Coomassie staining). Values were calculated using the image processing package Fiji [60].

	WT	p27$^{-/-}$	p27OE	p27$^{-/-}$AB
880kDa band	0.682	0.792	0.754	1.264

Oxygen consumption and p27

In face of the results obtained in the BN-PAGE, we decided to measure oxygen consumption in all the strains in both promastigotes and amastigotes, to better assess the impact of p27 on the respiratory chain function. Basal oxygen consumption was measured using a Clark-type oxygen electrode. An example of the type of graph obtained is provided in figure 17.

In promastigotes, oxygen consumption was halted by adding KCN, a complex IV inhibitor, to confirm complex IV specificity. In the case of amastigotes, after measuring basal oxygen consumption, complex III was inhibited by the addition of

antimycin A, and the signal was close to zero. After stabilization of the signal, substrates for complex IV, ascorbate and TMPD were added to determine complex IV activity. TMPD acts as an electron carrier which is reduced by ascorbate and oxidized by complex IV, allowing for the measurement of complex IV activity.

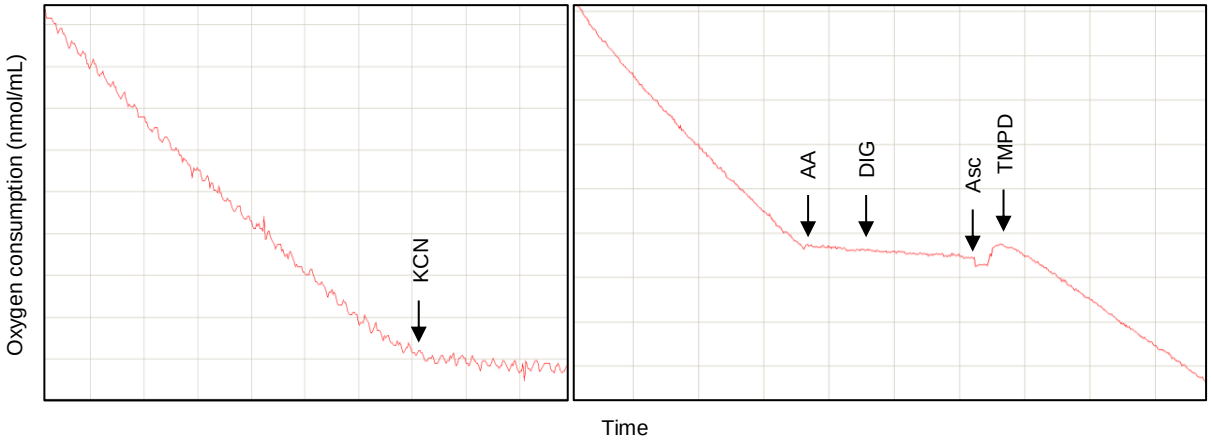

Figure 17. Oxygen consumption in p27$^{-/-}$ parasites. Representative assay of basal oxygen consumption by promastigotes followed by inhibition with 1mM of KCN (left graph). Right graph refers to a representative assay of basal oxygen consumption by amastigotes followed by antimycin A (AA) inhibition and permeabilization with digitonin (DIG). After signal stabilization, ascorbate (Asc) and TMPD were added to determine complex IV activity.

As shown in the left graph of figure 18a, all the strains of promastigotes have identical basal oxygen consumption and are inhibited by KCN at similar levels. No significant differences were found. On the contrary, p27$^{-/-}$ amastigotes have significantly higher basal and ascorbate/TMPD oxygen consumption rates than all the other strains (figure 18b, left graph). A western blot was performed with the same samples to check for the abundance of p27 in each strain (figure 19). As expected, p27$^{-/-}$ had no signal, while the p27OE had the most intense band.

Small variations are observed between basal oxygen consumption and after the addition of ascorbate and TMDP. These differences could be explained by the inherent variability of the assays and parasites or insufficient/excess permeabilization of the plasma membrane of the parasites by digitonin. Nonetheless, from these results it is possible to conclude that p27$^{-/-}$ amastigotes consume more oxygen than any of the strains tested, suggesting a regulatory role for p27 in decreasing complex IV activity.

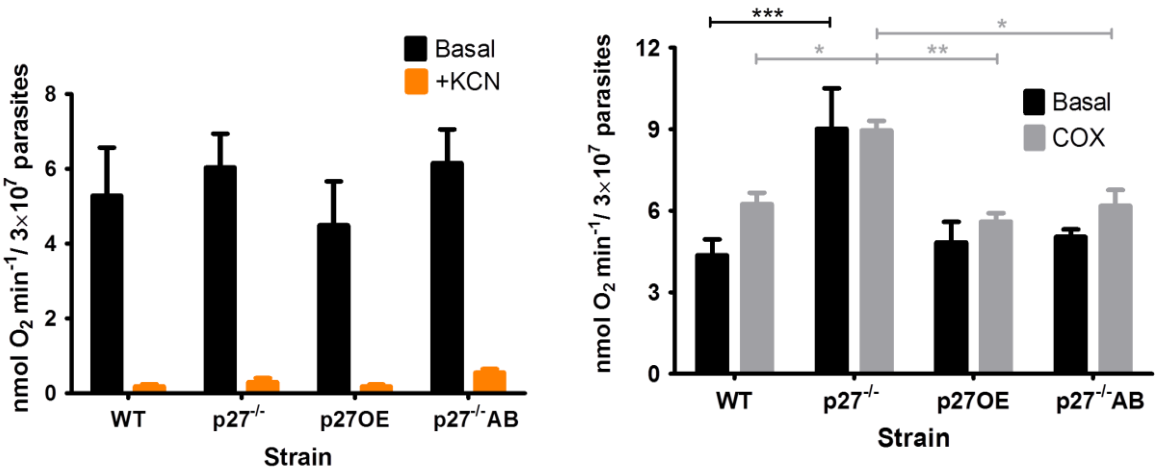

Figure 18. Oxygen consumption by *L. infantum* promastigotes (left graph) and amastigotes (right graph). Black bars represent basal oxygen consumption. Orange bars in the left graph indicate oxygen consumption after the addition of KCN. Grey bars in the right graph represent ascorbate/TMPD-dependent oxygen consumption. Results are represented as mean ± SEM.
* P<0.05; ** P<0.01 *** P<0.001

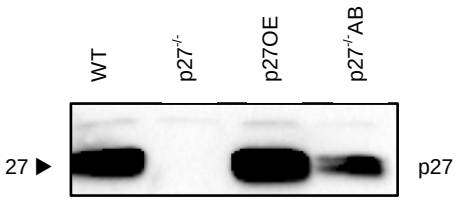

Figure 19. Western blot analysis of p27 expression in each amastigote strain used in oxygen consumption experiments. Number on the left indicates the molecular weight in kDa. The protein detected is identified on the right. The same number of parasites was loaded into each lane therefore, the quantity of protein is similar

Discussion

The activity of complex IV is crucial for an efficient electron transport that, ultimately, allows the production of ATP. A deeper understanding of mitochondrial function could be a big step to unravel the mechanisms by which *Leishmania* is able to infect, survive and thrive in a vertebrate host.

Initially, we searched and compared protein sequences of COX subunits of three different species (*L. infantum*, *T. brucei* and *M. musculus*) in different databases. Although the sequences of COX subunits are relatively conserved among trypanosomatids they do not have known counterparts in mammalian subunits, showing very low homology or none at all, indicating that complex IV of *L. infantum* is highly divergent of mammals. A previous study reached a similar conclusion after comparing sequences of COX subunits of humans and yeast against the ones of *T. brucei*. They found that only 2 subunits, COXVI (Tb10.100.0160) and COXVIII (Tb927.4.4620) shared some similarity with humans (subunits VIb and IV) and yeast (COX12 and COX5) [62].

During the present *in silico* study, 11 subunits were uncovered in *L. infantum*. The same number of subunits had been previously identified for *L. tarentolae* but these were only the nuclear encoded ones [63]. The three mitochondrial encoded subunits (COXI, COXII and COXIII) are predicted in some trypanosomatids but were never detected [64,65]. *L. infantum* is one of the species without known sequences of mitochondrial encoded subunits, since we were unable to find them in the databases TritrypDB, UniProt and PubMed. Therefore, the information regarding these subunits, provided in table 4, refers to *T. brucei*. The reason for this difficulty in experimentally detect the mitochondrial encoded subunits is a result of their high hydrophobicity, non-migration in SDS-PAGE gels and difficult peptide identification by mass spectrometry due to the lack of cleavage sites for trypsin [62].

Protein p27 is nuclear-encoded and only found in trypanosomatids along with another protein of similar size and sequence, protein p28. This protein doesn't seem to be recognized by the α-p27 antibody otherwise a band should be visible in the $p27^{-/-}$ samples. Sometimes a higher molecular weight band appears in some blots, and its presence didn't seem to be related with the strain, age of the parasites or stage of differentiation. We initially hypothesized that this could be p28 but quickly discarded this idea since p28 and p27 have almost the same molecular weight (27843 and 27633 Da, respectively), thus the band is probably not specific.

The two proteins, p27 and p28, could be isoforms (figure 7). Isoforms of subunits of complex IV are present and described in mammals. For example, some isoforms have varying abundance in the different tissues and could be induced by different stimuli [66]. Similarly, p27 begins to be expressed when the temperature increases and pH decreases and, therefore, is mostly expressed in amastigotes growth conditions. However, information about p28 expression is even scarcer than p27 and the data that we obtained is insufficient to confirm this hypothesis. Further studies concerning p27 and p28 are necessary to clarify this issue.

Since no solved p27 protein exists in PDB the continuation of the *in silico* will hardly give us clues on p27's function. So, the next step was to eliminate p27 as a way to obtain more information about it, though knocking-out genes is often challenging in *Leishmania* because of limited iRNA machinery [67] and the plasticity in chromosome number [68]. Fortunately, the CRISPR-Cas9 system was recently adapted to kinetoplastids [56] and has proved to be an effective method to easily knock-out genes, facilitating the study of many aspects of *Leishmania* biology.

In this work this was no exception, since *L. infantum* clones devoid of p27 ($p27^{-/-}$ parasites) were quickly isolated and had no major differences in growth or morphology (figure 10). In fact, strains WT, $p27^{-/-}$, p27OE and $p27^{-/-}$AB were indistinguishable as promastigotes and as amastigotes, the only exception being $p27^{-/-}$ amastigotes, which had a slightly diminished culture density. This indicates that p27 is not essential for parasite survival in axenic cultures. p27OE and $p27^{-/-}$AB promastigotes present ectopic copies (pGL.BSD.p27 and pGL.Hyg.p27 plasmids, respectively) of p27 ORF, and we have confirmed expression of p27 in logarithmic phase parasites. Nonetheless, p27 was not detected in stationary phase parasites. Since, p27 is a protein only expressed in amastigotes it might have some toxic effect in stationary promastigotes that degraded p27.

We determined that p27 starts to be expressed relatively early in the differentiation process and increases progressively (figure 12). At 24h (when the first signal appears) parasites have a more amastigote-like appearance, while in the earlier time-points (6 and 12h) they are more oval and still retain the flagellum. This could suggest a possible role for p27 in parasite differentiation, however, the presence or absence of p27 does not seem to compromise the parasites' ability to differentiate, since all the strains were successfully differentiated into amastigotes.

Neither of the strains seemed to have an impaired capability to infect and survive in macrophages (figure 14). In fact, p27OE was the most virulent strain with the highest percentages of infection and number of parasites per cell, which suggests that

the excess of p27 makes parasites more virulent. Even so, if this was the case, we should expect a lower infection percentage and number of parasites in macrophages infected with p27$^{-/-}$. Instead, we observe that WT, p27$^{-/-}$ and p27$^{-/-}$AB all have identical percentages of infection. Contrary to our results, previous studies in *L. donovani* and *L. major* [2,54], showed that p27$^{-/-}$ parasites, although able to infect macrophages, had very low percentages of infection that decreased throughout time suggesting a reduction in parasite virulence when p27 is absent. However, the study with *L. donovani* was conducted in a different manner (e.g. the use of human macrophages and intramacrophagic amastigotes), which could explain the different results.

In our *in vivo* experiments, p27$^{-/-}$ parasites do not seem to proliferate neither in the spleen nor liver (figure 15). The same result was described previously for p27$^{-/-}$ parasites from both *L. donovani* and *L. major* [2,54], and the reasons for the low proliferation and virulence were tentatively attributed to a reduction of ATP production by oxidative phosphorylation due to an impaired complex IV in the mutant strains. Although we didn't measure ATP production, we quantified complex IV activity in axenic amastigotes and observed that in the p27$^{-/-}$ parasites the activity was higher than that of WT parasites or even p27OE parasites (figure 16 and table 6).

This result was further supported by measuring oxygen consumption rates (figure 18). As expected, promastigotes had no significant differences in their basal oxygen consumption, since p27 is not naturally expressed during this stage of their life cycle. However, in amastigotes, significant differences were found, with p27$^{-/-}$ parasites displaying higher basal and ascorbate/TMPD-dependent oxygen consumption rates than any of the other strains, indicating that in *L. infantum* p27 has a role in regulating complex IV activity by decreasing it. The p27$^{-/-}$AB parasite line displayed oxygen consumption rates that were similar to the ones of WT, however, they had higher levels of in-gel COX activity (figure 16). Although these p27$^{-/-}$AB parasites abundantly express p27 as amastigotes (as we previously showed, figure 13 and 19) in the BN-PAGE sample, p27 was not expressed, since no 880kDa band was detected with the α-p27 antibody (figure 16c). It is also important to mention that these analyses have only been done once and need to be repeated to clarify this issue. In the case of p27OE parasites, the protein was abundantly expressed (figure 13 and 19) and was found associated to complex IV which resulted in an activity level similar to WT and lower than in p27$^{-/-}$.

Besides the 880kDa band corresponding to complex IV, we observed a second band of approximately 440kDa with in-gel COX activity and detected by the α-p27 antibody (figure 16). This 440kDa band is increased in p27$^{-/-}$ and p27$^{-/-}$AB strains. It

appears that the complex partially disassociated into a 440kDa component that still exhibits some COX activity, and p27, when present, is found associated with it or this 440kDa assembly is the monomer of the enzyme. This observation suggests a role for p27 in stabilizing complex IV. The presence of two bands could indicate that complex IV is a dimer, which would explain the discrepancy between the sum of all the subunits encountered in the *in silico* assay (roughly 300kDa) and the size of the band corresponding to complex IV in the in-gel activity assay. Even so, the list (table 4) presented in this work is almost certainly incomplete and many subunits are likely to have remained unidentified.

In summary, we obtained some puzzling results because $p27^{-/-}$ parasites have higher COX activity as well as oxygen consumption rates, and yet they are not able to proliferate in mice. Initially, we hypothesized that p27 could be helping in the stabilization of complex IV in response to high temperatures. *Leishmania* expresses a series of heat-shock proteins that can form chaperone complexes to coordinate responses to heat shock and promastigote-amastigote differentiation [69]. This hypothesis would agree with our observation that p27 expression augments more when the temperature increased than when pH decreased (figure 13), suggesting that temperature is an important environmental cue. However, this does not seem to be the only function of p27 since its depletion increases COX activity along with a low proliferation rate *in vivo*.

Another explanation is that protein p28, due to its similarity with p27, could be compensating for the absence of p27 in the $p27^{-/-}$ parasites. Expression of p28 assures stability and increases COX activity, explaining the absence of a phenotype in axenic cultures without being able to compensate $p27^{-/-}$ *in vivo* phenotype. However, we have no indications that p28 is expressed in amastigotes and neither that it associates with complex IV and therefore, further studies are needed to test this hypothesis.

In an attempt to decipher the conundrum referred to above we turned our attention to the relation between host and parasite and the amastigote metabolism. It has been proposed that amastigotes could enter a quiescent state as a strategy to survive in the vertebrate host [50]. Restricting one's own growth and metabolic activity might seem like a detrimental approach, yet it has a number of possible advantages. Namely, better protection from the high temperature and low pH experienced inside the PV, lower dependency in the ETC for the production of energy which could be inhibited by RNS/ROS and minimization of nutrient uptake preventing metabolic stress [50].

So, in a way *Leishmania* reduces its pathogenicity, which allows it to remain for longer periods of time in the host. As any other living being, a parasite tries to exploit

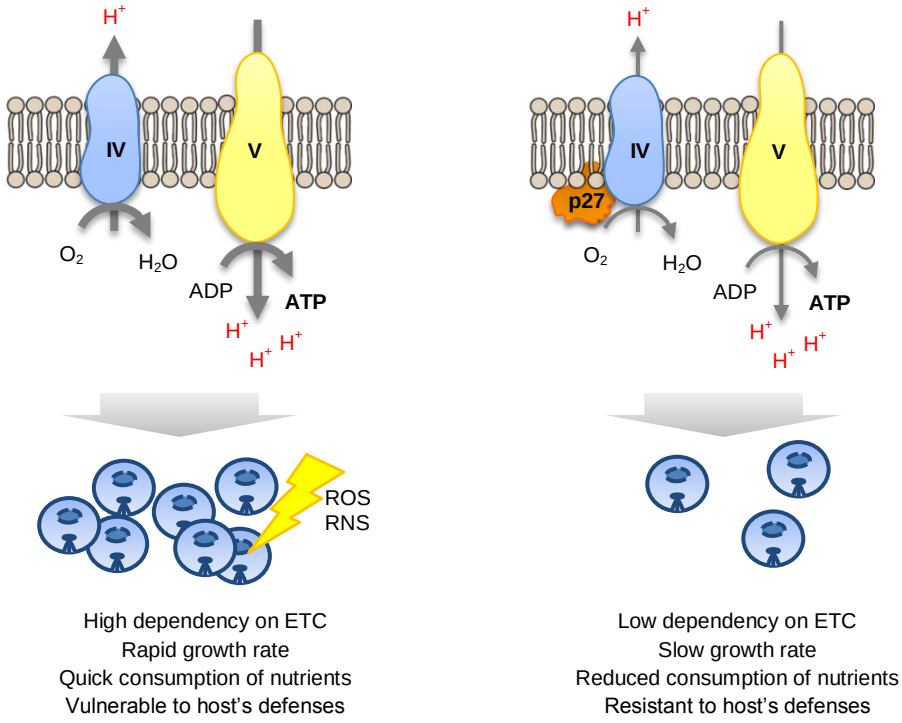

Figure 20. Graphical summary of the possible mechanism of action of p27 and its consequences in parasite virulence. Blue circles represent amastigotes. Abbreviations: ADP, adenosine diphosphate, ATP, adenosine triphosphate; RNS, reactive nitrogen species, ROS, reactive oxygen species; ETC, electron transport chain
Scheme made in part with images from https://smart.servier.com/

the environment as best as possible to survive, and a severe infection frequently limits the host's ability to feed, move and reproduce which in turn could compromise transmission and disrupt the parasite's life cycle [70].

The protein p27 could be contributing to the establishment of this quiescent state by reducing the activity of complex IV and, consequently, the production of ATP by oxidative phosphorylation. Moreover, p27 expression could also modify ROS production. So, $p27^{-/-}$ parasites have higher COX activity, but at the same time, are unable to proliferate in the vertebrate host because they are more susceptible to the action of ROS and RNS and/or nutrient scarcity. In figure 20 a graphical summary of this proposed hypothesis is presented.

A comparable situation can be found in hematopoietic stem cells (HSCs). HSCs repress mitochondrial oxidative metabolism, which promotes quiescence. When mitochondrial biogenesis is promoted, ROS and ATP production increases, quiescence is abandoned, HSCs start to proliferate and become more sensitive to differentiation stimuli. Therefore, regulation of mitochondrial metabolism and quiescence maintenance are strongly connected [71,72]. Amastigotes, like HSCs, could be

maintained at relatively constant numbers, at least in the spleen, where the infection persists for long periods of time. The effect of p27 is only obvious later in the infection, since no differences were observed in *in vitro* assays and at the 7th day p.i. in the spleen of infect mice. It's possible that, in mice, amastigotes initially proliferate and are later contained by some stimuli from the host (e.g. temperature, ROS/RNS). In such scenario, p27 would have no impact on the parasite's ability to infect cells but would be essential for the progression of the infection.

Establishing a quiescent state to better endure a harsher environment is by no means exclusive of *Leishmania* or even trypanosomatids. All organisms (parasite or free-living) are subjected to a constantly changing environment, and periods of scarcity and stress are part of it [73]. Many bacteria (e.g. *Mycobacterium tuberculosis*, *Brucella abortus* and *Staphylococcus aureus*) are able to persist in a host regardless of antibiotic treatment. This is often associated with slow growth and a decrease in metabolic activity [74]. Fungi, like the yeast *Saccharomyces cerevisiae*, are also able to enter quiescent state where there's no replication, protein synthesis is reduced and resistance to heat and toxic compounds is increased [75]. Some viruses can also persist in a host, often for the rest of its life, as it is the case of the herpes virus. The virus survives inside nerve cells in a dormant state with only occasional reactivation to produce more viruses [76].

Regardless of the microbe, one common feature in cellular quiescence is carbon storage. *S. cerevisiae* accumulates glycogen, trehalose, and triglycerides [75]. Bacteria usually accumulate lipids (mainly in the form of fatty acids) [77] and *Leishmania* stores mannan, especially as amastigotes, were it constitutes up to 90% of the cellular carbohydrates [78]. Conversely, promastigotes accumulate either very low levels or no mannan. The mannan levels increase radically when parasites are subject to acidic pH and high temperature (conditions experienced inside macrophages). The accumulation of carbon appears to function as an energy reserve that is used during differentiation and in establishment of infection [78]. We didn't quantify mannan levels in either of the strains, although we speculate that p27$^{-/-}$ could be consuming these important reserves at a faster rate than WT parasites, leading to a rapid depletion of nutrients and, subsequently, a low proliferation *in vivo*. It would be interesting to see if there are any differences in carbon storage among the different strains.

Nonetheless, it is difficult to envisage how *L. infantum* p27$^{-/-}$ would have more complex IV activity, while related species like *L. donovani* (also a VL causal agent) and *L. major* displayed decreased activity associated with reduced proliferation. The reasons for this discrepancy remain unclear. Nevertheless, and as described

previously, different species of *Leishmania* cause very different types of disease in a host (from fatal disease to asymptomatic) and the reasons for these different outcomes are also poorly understood. Thus, it is possible that major differences in the metabolic profile of parasites (even closely related ones) should occur. Notwithstanding, it is also important to acknowledge that the results presented here are still preliminary and require further confirmation and study.

The fact remains that there's still a lot to uncover regarding amastigote metabolism, since most of the studies conducted are performed in *in vitro* cultivated promastigotes. Establishing axenic amastigotes cultures is challenging, and in the case of some species impossible, and this constitutes a significant obstacle in the study of these parasites. New techniques and optimization of existing protocols need to be considered to facilitate future investigations into the complex mitochondrial metabolism of *Leishmania* amastigotes.

Future perspectives

The energy metabolism of *Leishmania* is a perplexing matter with multiple pathways and variables affecting it. Discovering these intricate mechanisms is essential to find new treatment options for leishmaniasis. This could be accomplished by creating a vaccine or targeting pathways and proteins unique to this parasite avoiding the toxic effects of many drugs used today.

First of all, it is necessary to repeat the BN-PAGE and the oxygen consumption experiments, since these are preliminary results that need further validation. Alternatively, enzymatic function of complex IV could also be measured by other protocols. Furthermore, evaluation of complex IV activity in intramacrophagic amastigotes is crucial to understand the effect of p27 deletion in enzyme function in a more physiological situation.

To better dissect the role of p27 and similar proteins in the pathogenicity of *Leishmania* it would be important to determine its 3D structure which could provide some clues about its function. To accomplish this, protein purification and subsequent X-ray crystallography would be necessary.

Longer post-infection time-points should be made to confirm if $p27^{-/-}$ parasites are fully eliminated from the host or can persist in the infected organs. Earlier time-points post-infection could reveal if $p27^{-/-}$ parasites proliferate rapidly in the first days of infection and are later contained as our hypothesis predicts. Also measurement of the levels of cytokines along the infection in mice to better assess the role of the host's immune system in the containment of the parasite.

The strains p27OE and $p27^{-/-}$AB should also be included in future *in vivo* experiments. The $p27^{-/-}$AB strain is essential to confirm that the phenotype observed for the $p27^{-/-}$ parasites is indeed the result of p27 ablation and not due to an off target effect of the CRISPR-Cas system. Depending on the results, we might have to complement the knockout parasites by integration of p27 ORF in the genome instead of expressing p27 from an episome

Investigate the ability of $p27^{-/-}$ parasites to actively replicate in macrophages from infected organs or if they remain in a latent state with little or no multiplication (possibly through a BrdU incorporation assay [79]). This could lead to the identification of pathways essential for the quiescent state of amastigotes.

It would also be interesting to see how the expression of p27 varies along infection. We tried to perform this experiment but the protocol followed was not ideal.

Thus, optimization of *Leishmania* protein extraction from infected macrophages is necessary in order to obtain robust results. Similar assays could also be done in infected mice upon collection of the spleen and liver.

Finally, it would be interesting to further explorer the protein p28 by doing a similar battery of experiments as in p27: checking if there's differential expression, if it's a mitochondrial membrane protein and a COX subunit and the impact of its absence in parasite survival.

References

1. Pace, D. Leishmaniasis. *World Health Organization* **69,** S10–S18 (2018).

2. Dey, R. *et al.* Characterization of a Leishmania stage-specific mitochondrial membrane protein that enhances the activity of cytochrome c oxidase and its role in virulence. *Mol. Microbiol.* **77,** 399–414 (2010).

3. Ferreira, W. F. C., Sousa, J. C. F. & Lima, N. *Microbiologia*. (Lidel, 2010).

4. David Sibley, L. Invasion and intracellular survival by protozoan parasites. *Immunol. Rev.* **240,** 72–91 (2011).

5. Ren, B. & Gupta, N. Taming Parasites by Tailoring Them. *Front. Cell. Infect. Microbiol.* **7,** 1–7 (2017).

6. Epidemiology & Risk Factors. *Centers for Disease Control and Prevention* (2013). Available at: https://www.cdc.gov/parasites/leishmaniasis/epi.html. (Accessed: 16th August 2017)

7. Hommel, M. Visceral leishmaniasis: biology of the parasite. *J. Infect.* **39,** 101–111 (1999).

8. Bates, P. A. The developmental biology of Leishmania promastigotes. *Experimental parasitology* **79,** 215–8 (1994).

9. Podinovskaia, M. & Descoteaux, A. *Leishmania* and the macrophage: a multifaceted interaction. *Future Microbiol.* **10,** 111–129 (2015).

10. Blander, J. M. & Medzhitov, R. On regulation of phagosome maturation and antigen presentation. *Nat. Immunol.* **7,** 1029–1035 (2006).

11. Moradin, N. & Descoteaux, A. Leishmania promastigotes: building a safe niche within macrophages. *Front. Cell. Infect. Microbiol.* **2,** 1–7 (2012).

12. Bogdan, C., Gessner, A., Werner, S. & Martin, R. Invasion, control and persistence of Leishmania parasites. *Curr. Opin. Immunol.* **8,** 517–525 (1996).

13. Kaye, P. & Scott, P. Leishmaniasis: complexity at the host–pathogen interface. *Nat. Rev. Microbiol.* **9,** 604–615 (2011).

14. Desjeux, P. Human leishmaniases: epidemiology and public health aspects. *World Heal. Stat Q* **45,** 267–275 (1992).

15. Campino, L. & Maia, C. Epidemiologia das leishmanioses em Portugal. *Acta Med. Port.* **23,** 859–864 (2010).

16. Alvar, J. *et al.* The relationship between leishmaniasis and AIDS: The second 10 years. *Clin. Microbiol. Rev.* **21,** 334–359 (2008).

17. Campino, L. *et al.* Leishmaniasis in Portugal: Enzyme polymorphism of Leishmania infantum based on the identification of 213 strains. *Trop. Med. Int. Heal.* **11,** 1708–1714 (2006).

18. Dunning, N. Leishmania vaccines: from leishmanization to the era of DNA technology. *Biosci. Horizons* **2,** 73–82 (2009).

19. McCall, L. I., Zhang, W. W., Ranasinghe, S. & Matlashewski, G. Leishmanization revisited: Immunization with a naturally attenuated cutaneous Leishmania donovani isolate from Sri Lanka protects against visceral leishmaniasis. *Vaccine* **31,** 1420–1425 (2013).

20. Engwerda, C. R., Ato, M. & Kaye, P. M. Macrophages, pathology and parasite persistence in experimental visceral leishmaniasis. *Trends Parasitol.* **20,** 524–530 (2004).

21. Rodrigues, V., Cordeiro-Da-Silva, A., Laforge, M., Silvestre, R. & Estaquier, J. Regulation of immunity during visceral Leishmania infection. *Parasites and Vectors* **9,** 1–13 (2016).

22. Stanley, A. C. & Engwerda, C. R. Balancing immunity and pathology in visceral leishmaniasis. *Immunol. Cell Biol.* **85,** 138–147 (2007).

23. Singh, O. P., Hasker, E., Sacks, D., Boelaert, M. & Sundar, S. Asymptomatic leishmania infection: A new challenge for leishmania control. *Clin. Infect. Dis.* **58,** 1424–1429 (2014).

24. Michel, G., Pomares, C., Ferrua, B. & Marty, P. Importance of worldwide asymptomatic carriers of Leishmania infantum (L. chagasi) in human. *Acta Trop.* **119,** 69–75 (2011).

25. Moshfe, A. *et al.* Canine visceral leishmaniasis: Asymptomatic infected dogs as

a source of L. infantum infection. *Acta Trop.* **112,** 101–105 (2009).

26. Svobodová, M., Votýpka, J., Nicolas, L. & Volf, P. Leishmania tropica in the black rat (Rattus rattus): Persistence and transmission from asymptomatic host to sand fly vector Phlebotomus sergenti. *Microbes Infect.* **5,** 361–364 (2003).

27. Dehio, C., Berry, C. & Bartenschlager, R. Persistent intracellular pathogens. *FEMS Microbiol. Rev.* **36,** 513–513 (2012).

28. Tielens, A. G. M. & van Hellemond, J. J. Surprising variety in energy metabolism within Trypanosomatidae. *Trends Parasitol.* **25,** 482–490 (2009).

29. Opperdoes, F. R. & Coombs, G. H. Metabolism of Leishmania: proven and predicted. *Trends Parasitol.* **23,** 149–158 (2007).

30. Saunders, E. C. *et al.* Central carbon metabolism of Leishmania parasites. *Parasitology* **137,** 1303–1313 (2010).

31. Bringaud, F., Rivière, L. & Coustou, V. Energy metabolism of trypanosomatids: Adaptation to available carbon sources. *Mol. Biochem. Parasitol.* **149,** 1–9 (2006).

32. Rosenzweig, D. *et al.* Retooling Leishmania metabolism: from sand fly gut to human macrophage. *FASEB J.* **22,** 590–602 (2008).

33. Rodriguez-Contreras, D., Feng, X., Keeney, K. M., Bouwer, H. G. A. & Landfear, S. M. Phenotypic characterization of a glucose transporter null mutant in Leishmania mexicana. *Mol. Biochem. Parasitol.* **153,** 9–18 (2007).

34. Haanstra, J. R. *et al.* Compartmentation prevents a lethal turbo-explosion of glycolysis in trypanosomes. *Proc. Natl. Acad. Sci. U. S. A.* **105,** 17718–23 (2008).

35. Haanstra, J. R., González-Marcano, E. B., Gualdrón-López, M. & Michels, P. A. M. Biogenesis, maintenance and dynamics of glycosomes in trypanosomatid parasites. *Biochim. Biophys. Acta - Mol. Cell Res.* **1863,** 1038–1048 (2016).

36. Fidalgo, L. M. & Gille, L. Mitochondria and trypanosomatids: Targets and drugs. *Pharm. Res.* **28,** 2758–2770 (2011).

37. de Souza, W., Attias, M. & Rodrigues, J. C. F. Particularities of mitochondrial structure in parasitic protists (Apicomplexa and Kinetoplastida). *Int. J. Biochem.*

Cell Biol. **41,** 2069–2080 (2009).

38. Tielens, A. G. M. & Van Hellemond, J. J. Differences in energy metabolism between Trypanosomatidae. *Parasitol. Today* **14,** 265–271 (1998).

39. Tielens, A. G. M. New functions for parts of the Krebs cycle in procyclic Trypanosoma brucei, a cycle not operating as a cycle. *Biochemistry* **280,** 12451–12460 (2005).

40. Mcconville, M. J. & Naderer, T. Metabolic Pathways Required for the Intracellular Survival of Leishmania. (2011). doi:10.1146/annurev-micro-090110-102913

41. Cazzulo, J. J. Aerobic fermentation of glucose by trypanosomatids. *FASEB J.* **6,** 3153–3161 (1992).

42. Van Hellemond, J. J., Van Der Meer, P. & Tielens, A. G. M. Leishmania infantum promastigotes have a poor capacity for anaerobic functioning and depend mainly on respiration for their energy generation. *Parasitology* **114,** 351–360 (1997).

43. Santhamma, K. R. & Bhaduri, A. Characterization of the respiratory chain of Leishmania donovani promastigotes. *Mol. Biochem. Parasitol.* **75,** 43–53 (1995).

44. Ferrier, D. R. *Lippincott's Illustrated Reviews: Biochemistry*. (Lippincott Williams & Wilkins, 2011).

45. Duarte, M. & Tomás, A. M. The mitochondrial complex I of trypanosomatids - An overview of current knowledge. *J. Bioenerg. Biomembr.* **46,** 299–311 (2014).

46. Clarkson, A. B., Bienen, E. J., Pollakis, G. & Grady, R. W. Respiration of bloodstream forms of the parasite Trypanosoma brucei brucei is dependent on a plant-like alternative oxidase. *J. Biol. Chem.* **264,** 17770–17776 (1989).

47. McConville, M. J., de Souza, D., Saunders, E., Likic, V. A. & Naderer, T. Living in a phagolysosome; metabolism of Leishmania amastigotes. *Trends Parasitol.* **23,** 368–375 (2007).

48. Saunders, E. C. *et al.* Induction of a Stringent Metabolic Response in Intracellular Stages of Leishmania mexicana Leads to Increased Dependence on Mitochondrial Metabolism. *PLoS Pathog.* **10,** (2014).

49. Naderer, T. & McConville, M. J. Intracellular growth and pathogenesis of Leishmania parasites. *Essays Biochem.* **51,** 81–95 (2011).

50. McConville, M. J., Saunders, E. C., Kloehn, J. & Dagley, M. J. Leishmania carbon metabolism in the macrophage phagolysosome - feast or famine? *F1000Research* **4,** 1–11 (2015).

51. Alcolea, P. J. *et al.* Transcriptomics throughout the life cycle of Leishmania infantum: High down-regulation rate in the amastigote stage. *Int. J. Parasitol.* **40,** 1497–1516 (2010).

52. Dey, R. *et al.* Live attenuated Leishmania donovani p27 gene knockout parasites are nonpathogenic and elicit long-term protective immunity in BALB/c mice. *J. Immunol.* **190,** 2138–49 (2013).

53. Avishek, K. *et al.* Gene deleted live attenuated Leishmania vaccine candidates against visceral leishmaniasis elicit pro-inflammatory cytokines response in human PBMCs. *Sci. Rep.* **6,** 4–13 (2016).

54. Elikaee, S. *et al.* Development of a new live attenuated Leishmania major p27 gene knockout: Safety and immunogenicity evaluation in BALB/c mice. *Cell. Immunol.* 0–1 (2018). doi:10.1016/j.cellimm.2018.07.002

55. Sharma, P., Gurumurthy, S., Duncan, R., Nakhasi, H. L. & Salotra, P. Comparative in vivo expression of amastigote up regulated Leishmania genes in three different forms of Leishmaniasis. *Parasitol. Int.* **59,** 262–264 (2010).

56. Beneke, T. *et al.* A CRISPR Cas9 high-throughput genome editing toolkit for kinetoplastids. *R. Soc. Open Sci.* **4,** 170095 (2017).

57. Schumann Burkard, G., Jutzi, P. & Roditi, I. Genome-wide RNAi screens in bloodstream form trypanosomes identify drug transporters. *Mol. Biochem. Parasitol.* **175,** 91–94 (2011).

58. Salomé Gomes, M. *et al.* Engagement of Toll-like receptor 2 in mouse macrophages infected with Mycobacterium avium induces non-oxidative and TNF-independent anti-mycobacterial activity. *Eur. J. Immunol.* **38,** 2180–2189 (2008).

59. Gomes-alves, A. G., Maia, A. F., Cruz, T., Castro, H. & Tomás, A. M. Development of an automated image analysis protocol for quantification of intracellular forms of Leishmania spp. *PLoS One* 1–15 (2018).

60. Schindelin, J. *et al.* Fiji: An open-source platform for biological-image analysis.

Nat. Methods **9,** 676–682 (2012).

61. Melo, A. M. P. *et al.* The External Calcium-dependent NADPH Dehydrogenase from Neurospora crassa Mitochondria *. **276,** 3947–3951 (2001).

62. Zíková, A. *et al.* Structural and functional association of Trypanosoma brucei MIX protein with cytochrome c oxidase complex. *Eukaryot. Cell* **7,** 1994–2003 (2008).

63. Horváth, A., Kingan, T. G. & Maslov, D. A. Detection of the mitochondrially encoded cytochrome c oxidase subunit I in the trypanosomatid protozoan Leishmania tarentolae: Evidence for translation of unedited mRNA in the kinetoplast. *J. Biol. Chem.* **275,** 17160–17165 (2000).

64. De la Cruz, V. F., Neckelmann, N. & Simpson, L. Sequences of six genes and several open reading frames in the kinetoplast maxicircle DNA of Leishmania tarentolae. *J. Biol. Chem.* **259,** 15136–15147 (1984).

65. Payne, M., Rothwell, V., Jasmer, D. P., Feagin, J. E. & Stuart, K. Identification of mitochondrial genes in Trypanosoma brucei and homology to cytochrome c oxidase II in two different reading frames. *Mol. Biochem. Parasitol.* **15,** 159–170 (1985).

66. Kadenbach, B. & Hüttemann, M. The subunit composition and function of mammalian cytochrome c oxidase. *Mitochondrion* **24,** 64–76 (2015).

67. Lye, L. F. *et al.* Retention and Loss of RNA interference pathways in trypanosomatid protozoans. *PLoS Pathog.* **6,** (2010).

68. Bastien, P., Blaineau, C. & Pages, M. Leishmania: Sex, lies and karyotype. *Parasitol. Today* **8,** 174–177 (1992).

69. Morales, M. A. *et al.* Phosphoproteome dynamics reveal heat-shock protein complexes specific to the Leishmania donovani infectious stage. *Proc. Natl. Acad. Sci.* **107,** 8381–8386 (2010).

70. Combes, C. Fitness of parasites: Pathology and selection. *Int. J. Parasitol.* **27,** 1–10 (1997).

71. Piccoli, C. & Capitanio, N. Mitochondria confirmed as drivers of HSC fate. *Blood* **132,** 878–880 (2018).

72. Hu, M. *et al.* SRC-3 is involved in maintaining hematopoietic stem cell quiescence by regulation of mitochondrial metabolism in mice. *Blood* **132,** blood-2018-02-831669 (2018).

73. Rittershaus, E. S. C., Baek, S. H. & Sassetti, C. M. The normalcy of dormancy: Common themes in microbial quiescence. *Cell Host Microbe* **13,** 643–651 (2013).

74. Fisher, R. A., Gollan, B. & Helaine, S. Persistent bacterial infections and persister cells. *Nat. Rev. Microbiol.* **15,** 453–464 (2017).

75. Gray, J. V *et al.* "'Sleeping Beauty"': Quiescence in Saccharomyces cerevisiae". *Microbiol. Mol. Biol. Rev.* **68,** 187–206 (2004).

76. Crawford, D. H. Persistent viruses. in *Viruses - A very short introduction* 65–82 (Oxford University Press, 2011).

77. Daniel, J., Maamar, H., Deb, C., Sirakova, T. D. & Kolattukudy, P. E. Mycobacterium tuberculosis uses host triacylglycerol to accumulate lipid droplets and acquires a dormancy-like phenotype in lipid-loaded macrophages. *PLoS Pathog.* **7,** (2011).

78. Ralton, J. E. *et al.* Evidence that Intracellular β1-2 Mannan Is a Virulence Factor in Leishmania Parasites. *J. Biol. Chem.* **278,** 40757–40763 (2003).

79. Mandell, M. A. & Beverley, S. M. Continual renewal and replication of persistent *Leishmania major* parasites in concomitantly immune hosts. *Proc. Natl. Acad. Sci.* 201619265 (2017). doi:10.1073/pnas.1619265114